

DESIGN CONSIDERATIONS IN MULTI-CARRIER CODE DIVISION
MULTIPLE ACCESS

by

GUY D. MARCHILDON

B. Eng., Royal Military College of Canada, 1991

A Thesis Submitted in Partial Fulfillment of the Requirements
for the Degree of


MASTER OF APPLIED SCIENCE

in the Department of Electrical and Computer Engineering


We accept this thesis as conforming
to the required standard




Dr. V. K. Bhargava, Dept. of Electrical & Computer Engineering



Dr. W. Little, Dept. of Electrical & Computer Engineering



Dr. B. Tabarrok, Dept. of Mechanical Engineering



Dr. R. Podhorodeski, External Examiner

© GUY D. MARCHILDON, 1998

University of Victoria

*All rights reserved. This thesis may not be reproduced in whole or in part by
photocopy or other means, without the permission of the author.*

Supervisor: Dr. V. K. Bhargava

ABSTRACT

A recently proposed multiple access scheme that combines the advantages of Orthogonal Frequency Division Multiplexing and Code Division Multiple Access has shown to have potential for application in the mobile radio environment. The purpose of this thesis is to investigate several design aspects of this scheme, which is called Multi-Carrier Code Division Multiple Access (MC-CDMA). The scheme is evaluated for the downlink (basestation to mobile receiver) of a single cell system using a typical bad urban mobile radio channel. The important system parameters are selected based on design requirements of high flexibility, good bit error rate performance, low crest factor, and low complexity. The investigation includes the selection of spreading codes, as well as the code length and the number of subcarriers. Following sections detail the interleaver design and the channel estimation technique chosen for the system simulations.


With the system design parameters selected an investigation into detection schemes is made. Conventional detection for MC-CDMA is performed by equalization in the frequency domain followed by a hard decision. Several detection schemes are compared through Monte Carlo simulations. Multi-user detection and maximum likelihood detection are then evaluated.

The issue of high crest factor is considered in conjunction with the frequency distribution of the transmitted MC-CDMA signal. Crest factor is a critical issue in multi-carrier systems in that high crest factor limits the system to the use of expensive amplifiers. Methods of reducing the crest factor for different detection schemes are investigated taking account of their effects on the frequency distribution. These methods are based on the use of phase rotations of the signal components. The issues addressed in this thesis provide groundwork for future development in the application of MC-CDMA in the mobile radio environment.

Examiners:




Dr. V. K. Bhargava, Dept. of Electrical & Computer Engineering



Dr. W. Little, Dept. of Electrical & Computer Engineering



Dr. B. Tabarrok, Dept. of Mechanical Engineering



Dr. R. Podhorodeski, External Examiner

Table of Contents

Abstract	ii
Table of Contents	iv
List of Figures	viii
List of Tables	x
Acknowledgement	xi
1 Introduction	1
1.1 Motivation	1
1.2 Current System Concept	1
1.3 History	2
1.4 Significance of Research	2
1.5 Thesis Outline	3
2 Background	4
2.1 The Mobile Radio Channel	4
2.1.1 Types of Fading	4
2.1.2 Fading due to multi-path time delay spread	4
2.1.3 Power Delay Profile	5
2.1.4 Coherence Bandwidth	6
2.1.4.1 Frequency Selective Fading	6
2.1.4.2 Flat Fading	7

2.1.5	Fading effects due to Doppler spread	7
2.1.6	Coherence Time	8
2.1.6.1	Fast Fading	8
2.1.6.2	Slow Fading	9
2.2	The Cellular Concept	9
2.2.1	Early Systems	9
2.2.2	Frequency Reuse	9
2.2.3	Interference	10
2.3	Ways To Improve Capacity	11
2.4	Multiple Access Schemes	12
2.4.1	FDMA	12
2.4.2	TDMA	14
2.4.3	CDMA	14
2.4.4	Narrowband and Wideband	14
2.5	Hybrid Multiple Access Schemes	15
2.5.1	DS-CDMA	15
2.5.2	OFDM	16
2.5.3	MC-CDMA	17
2.5.4	Principles of OFDM	17
2.5.5	Advantages of MC-CDMA	22
2.5.5.1	Compared to Direct Sequence DS-CDMA	22
2.5.5.2	Compared to C-OFDM	22
2.5.6	Definition of MC-CDMA	22
2.5.7	Implementation using FFT	23
2.6	The MC-CDMA signal	23
2.6.1	Spreading Codes	23
2.6.2	Transmission scheme	24

2.7	Advantages of MC-CDMA	28
2.7.1	Flexible data rates	28
2.7.2	Reduced multiple access interference	29
2.7.3	Multipath Fading Mitigation	29
2.7.4	Frequency diversity	29
3	MC-CDMA System Definition	30
3.1	System Bandwidth	30
3.1.1	Symbol Duration	30
3.1.2	Processing Gain	31
3.2	Guard Interval	31
3.3	Bad Urban Radio Channel	31
3.3.1	Channel Parameters	32
3.4	Number of Subcarriers	32
3.5	Frequency Diversity	32
3.5.1	Frequency Interleaving	34
3.5.2	Achievable Diversity	35
3.6	Spreading Code Length	35
3.6.1	Maximum Likelihood Detection	35
3.6.2	User Groups	37
3.7	Channel Sounding	38
3.7.1	Grid Design	40
3.8	System Parameters	42
4	Design Considerations	45
4.1	Detection Schemes	45
4.1.1	Orthogonality Restoration Combining	47
4.1.2	Inverse Detection	48

4.1.2.1	Equal Gain Combining	48
4.1.2.2	Maximum Ratio Combining	48
4.1.2.3	Controlled Equalization	49
4.1.2.4	Minimum Mean Squared Error (MMSE) Equalization	50
4.1.3	Interference Cancellation through Multi-User Detection	50
4.1.4	Maximum Likelihood Detection (MLD)	51
4.2	Simulation Results	53
4.2.1	Orthogonal Restoration Combining	53
4.2.2	Interference Cancellation	60
4.3	Summary	63
4.4	Channel Coding	63
4.5	Spreading Codes for Crest Factor Reduction	66
4.5.1	Phase Rotation	68
4.5.1.1	Phase Scrambling	72
4.6	Selected Mapping (SLM)	72
5	Conclusions and Suggestions for Further Work	76
5.1	Conclusions	76
5.2	Suggestions for Further Work	78
Bibliography		79

List of Figures

Figure 2.1	Illustration of the cellular frequency reuse concept. Cells with the same letter use the same set of frequencies. The bold line encloses a cell cluster which is replicated over the service coverage area.	10
Figure 2.2	In FDMA different channels are assigned to different frequencies. Guard intervals are inserted between frequencies.	13
Figure 2.3	In TDMA a channel occupies a time slot within a repetitive time frame. Guard times are required between time slots to minimize ISI.	13
Figure 2.4	In CDMA each channel is assigned a unique PN code which is orthogonal to other users PN codes.	13
Figure 2.5	Orthogonal spectra of OFDM signal.	17
Figure 2.6	Illustration of the cyclical extension of the MC-CDMA symbol to form the guard interval.	20
Figure 2.7	The effect of guard interval insertion.	21
Figure 2.8	Model of an MC-CDMA transmitter.	25
Figure 2.9	Model of an MC-CDMA receiver.	28
Figure 3.1	Instantaneous power delay profile for a COST bad urban channel.	33
Figure 3.2	BER for single user case and different spreading code lengths $l = 1, 2, 4, 8, 16, 32$	36
Figure 3.3	Illustration of the deterministic frequency interleaver employed with $Q=2, K=2$, and $L=4$	38
Figure 3.4	Performance improvement resulting from increased frequency diversity through block interleaving.	39
Figure 3.5	MC-CDMA frame with 512 subcarriers showing pilot tone placement with $N_l = 10$ and $N_k = 4$	41

Figure 3.6	The overall system configuration for the base station and the mobile user.	44
Figure 4.1	The MC-CDMA receiver	47
Figure 4.2	MC-CDMA receiver employing interference cancellation.	52
Figure 4.3	Decision curves for soft decision detection.	53
Figure 4.4	Results for inverse equalization (INV).	55
Figure 4.5	Results for Equal Gain Combining (EGC) equalization.	56
Figure 4.6	Results for Maximum Ratio Combining (MRC) equalization.	57
Figure 4.7	Results for Controlled Equalization (CE) with $\rho = 0.4$	58
Figure 4.8	Results for Minimum Mean Square Error (MMSE) equalization.	59
Figure 4.9	Results for Multi-User Detection (MUD) equalization.	61
Figure 4.10	A comparison of the best equalization schemes for system of varying complexity.	62
Figure 4.11	Rate 1/2, K=7, convolutionally encoded MC-CDMA with MLD and MMSE.	65
Figure 4.12	Applying phase rotation to spreading codes.	70
Figure 4.13	Normalized probability density function of Euclidean distances of received vectors about the transmitted vector.	71
Figure 4.14	Complimentary cumulative distribution function of CF if MC-CDMA symbol with lowest CF is selected out of M statistically independent symbols.	73
Figure 4.15	Complimentary cumulative distribution function of CF_{lowest} with M=1 and 4, D=512.	75

List of Tables

Table 1.1	Bit error rate and latency requirements of various data types.	2
Table 3.1	Channel parameters assumptions	42
Table 3.2	System parameters	43
Table 4.1	Normalized complexity and $BER = 10^{-3}$ performance of detection schemes	63

A c k n o w l e d g e m e n t

I would like to express my gratitude to Dr. Vijay K. Bhargava for the opportunities he has made available to his students and the vibrant atmosphere of the research lab he has created. Thanks to all of my friends in the Communications Research Lab and the other labs. Special thanks go to Dr. Michael Shnell, Lorenz Freiberg, and A. Annamalai for the guidance they have provided in this work. Finally, I would like offer my deepest thanks to friends and family, especially Nicole and my parents.

Chapter 1

Introduction

1.1 Motivation

The unprecedented growth of worldwide mobile wireless markets, along with the significant advances in wireless communication technologies and the accelerated development of interactive multimedia services are considered the main drivers of third-generation mobile wireless communication systems.

One significant challenge in the development of future mobile wireless networks will be the choice of an appropriate multiple access scheme. Third generation systems will require flexible multiple access schemes that can accommodate multiple data rates with high spectral efficiency, while using low complexity mobile receivers.

1.2 Current System Concept

The current system concept used at the International Telecommunication Union (ITU) for third generation cellular networks is referred to as IMT-2000 (International Mobile Telecommunications). Radio frequency allocations for IMT-2000 have been established everywhere except the USA which is currently deploying second generation networks in the same radio frequency. In Europe the Universal Mobile Telecommunication System (UMTS) bands will be in use starting in 2002. The IMT-2000 radio transmission techniques evaluation process has started, and submissions for candidate technologies are expected by October 1998 [1].

1.3 History

The Analog Mobile Phone System (AMPS) was the first wireless communication system to employ a cellular concept to achieve high system capacity. Introduced in 1983, the demand for these services rose rapidly and by the early 1990's a second generation of cellular systems (IS-54, IS-95, GSM) was introduced to overcome the capacity limitations of the analog systems [2]. These digital cellular systems offer low speed data capability in addition to voice.

We are now entering the era of third generation wireless communications. These networks will be required to provide not only voice and low speed data, but also a host of multimedia services to end users regardless of their locations. Essentially, all services offered by wireline networks will be expected to be matched in mobile form, although not necessarily at the same data rates. Providing these kinds of services over the hostile radio environment, under severe radio spectrum constraints, and at low user cost, is a considerable challenge. Table 1.1, derived from [3] presents some of the latency, bit error rate (BER), and data rate specifications for services that a next generation multi-media wireless network could be expected to provide.

Table 1.1. Bit error rate and latency requirements of various data types.

Data Type	Data Rate (kbps)	BER	Delay (sec)	Delay Jitter
Voice	4-30	10^{-3}	Critical	Critical
Facsimile	< 20	10^{-4}	Non-critical	Non-critical
Low resolution video	≈ 64	10^{-5}	Critical	Critical
Asynchronous packet data	< 20	10^{-9}	Non-critical	Non-critical
Synchronous packet data	8-128	10^{-9}	Critical	Critical

1.4 Significance of Research

The most critical step taken in the design of a mobile cellular communication system is the choice of multiple access scheme. Any new multiple access scheme proposed for these systems must be subjected to intense scrutiny to determine its suitability for the role. Multi-Carrier Code Division Multiple Access (MC-CDMA), proposed in 1994, is such a scheme [4]. Of particular importance is a signal design that maximizes spectral efficiency and capacity,

while accommodating multiple data rates, in a flexible and low cost manner.

The first objective of this thesis is to provide a framework on which a description of MC-CDMA can be based. Given this background material, an explanation of the MC-CDMA system, detailing its features and particular advantages over other techniques, can be given. We are then prepared to select specific parameters for a feasible MC-CDMA system; concentrating on achieving a signal design that meets the stated requirements of high capacity, flexibility, and low complexity. With a system design in place, several issues related to system performance are addressed. Namely, detection schemes that take full advantage of the frequency diversity offered by MC-CDMA are investigated with the aim of maximizing capacity. Next, some specific performance limiting aspects of MC-CDMA are addressed and improvements sought. These are the spreading code selection, crest factor reduction, and fading channel performance. These areas are very closely related and as such will be discussed together.

1.5 Thesis Outline

The five chapters of this thesis are as follows. Chapter 1 provides some background material as a means of introduction to the topic. Chapter 2 contains an overview of the urban mobile radio environment, from multi-path propagation to Doppler spreading, in order to later demonstrate the applicability of MC-CDMA to this channel. Our aim in Chapter 3 is to describe multi-carrier modulation. The chapter begins with a description of Orthogonal Frequency Division Multiplexing (OFDM) which forms the basis of MC-CDMA, proceeds with a brief description of the numerous other multi-carrier techniques recently introduced, and finally, a system description of MC-CDMA transceiver is presented. In Chapter 4 we focus on specific issues in MC-CDMA. Several detection schemes and interference cancellation techniques are simulated to compare capacity performance. Specifically, orthogonal restoration combining, multi-user detection, and maximum likelihood detection schemes are investigated. Channel coding is introduced as a means to detect and correct errors in the received signal. Considerations for the selection of spreading codes based on performance and complexity are then presented and a system for reducing crest factor in low complexity systems is introduced. The final chapter contains conclusions based on the simulations in Chapter 4, as well as several suggestions for future work in this field.

Chapter 2

Background

2.1 The Mobile Radio Channel

2.1.1 Types of Fading

A signal propagating through a mobile radio channel experiences two types of fading: large-scale and small-scale. Large scale fading represents the average signal power attenuation or path loss due to terrain contours over large propagation distances. Small-scale fading can result from two independent mechanisms: multi-path time delay spread and Doppler spread [2].

2.1.2 Fading due to multi-path time delay spread

Time delay spread results when a transmitted signal decomposes through multiple random reflections in the surrounding environment. Through these reflections, a signal can be seen to take many paths from the transmitter to the receiver. Each of these paths will experience attenuation and a time delay. The superposition of these paths at the receiver causes constructive and destructive interference of the original signal. It is this destructive interference that forms the single biggest obstacle to wireless communications. If there is no line of sight (LOS) component in the received signal, as is often the case in an outdoor environment over long distances, the received signal consists of scattered components due to reflections with no dominant path. The received signal can be separated into an in-phase and a quadrature component for each path [2]. The in-phase and quadrature signal components can be assumed to be zero-mean statistically independent Gaussian random variables by the Central Limit Theorem (CLT) with each having variance σ^2 . The envelope of the signal resulting from the vector addition of all components is Rayleigh distributed,

and the phase is uniformly distributed on the interval of $[0, 2\pi]$. The channel of interest in this thesis is the outdoor mobile channel which is generally characterized by Rayleigh fading. For the remainder of this thesis Rayleigh distributed fading will be assumed.

The probability density function (pdf) of a Rayleigh distributed random variable R is given by

$$p_R(r) = \begin{cases} \frac{r}{\sigma^2} e^{-\frac{r^2}{2\sigma^2}} & \text{if } r \geq 0 \\ 0 & \text{otherwise} \end{cases} \quad (2.1)$$

where r is the envelope amplitude of the received signal and $2\sigma^2$ is the pre-detection mean power of the multi-path signal. The mean and variance of the Rayleigh random variable are given by /citepro:digcomm

$$E_R[r] = \sqrt{\frac{\pi}{2}}\sigma \quad (2.2)$$

and

$$\sigma_r^2 = (2 - \frac{1}{2}\pi)\sigma^2 \quad (2.3)$$

It will be assumed that the propagating signal is in the ultra-high-frequency (UHF) band, encompassing present day cellular and planned future cellular network frequency allocations; around 1 GHz and 2 GHz respectively.

2.1.3 Power Delay Profile

A power delay profile can be used to characterize a mobile radio channel by telling us how the average received power of a transmitted pulse varies as a function of time delay. Maximum excess delay, mean excess delay, and (rms) delay spread, quantify the time dispersive properties of the power delay profile. The mean excess delay is the first moment of the power delay profile while the (rms) delay spread σ_τ is the square root of the second central moment of the power delay profile. In an urban area the rms delay spread ranges from 10 – 25 μs [2]. The maximum excess delay τ_{max} provides a measure of the time delay between the first detectable signal arriving at the receiver and the arrival of the last detectable echo.

2.1.4 Coherence Bandwidth

A completely analogous characterization of signal dispersion can be made in the frequency domain. The coherence bandwidth B_c of a channel is a relation derived from the rms delay spread, and is approximately

$$B_c \approx \frac{1}{\sigma_\tau} \quad (2.4)$$

Coherence bandwidth is a statistical measure of the range of frequencies over which the channel can be considered to pass all spectral components with approximately equal gain and linear phase. Put another way, coherence bandwidth is the range of frequencies over which two frequency components have a strong potential for amplitude correlation. If we consider the coherence bandwidth as the bandwidth over which the frequency correlation function is above 0.5, the coherence bandwidth is approximately [5].

$$B_c \approx \frac{1}{5\sigma_\tau} \quad (2.5)$$

It must be stressed that this expression is an approximation and that analysis of the specific channel on a specific signal are required to determine the exact effects of multi-path propagation. In a fading channel the relationship between maximum excess delay time τ_{max} and symbol time T_s , result in frequency-selective fading or frequency non-selective fading of the transmitted signal. Alternatively, in the frequency domain, the relationship between the coherence bandwidth B_c and the signal bandwidth B_s will result in frequency-selective fading or frequency non-selective fading of the transmitted signal.

2.1.4.1 Frequency Selective Fading

A channel experiences frequency-selective fading if

$$\sigma_\tau > T_s \quad (2.6)$$

and

$$B_s > B_c \quad (2.7)$$

This condition occurs whenever the received multi-path components of a symbol extend beyond the symbol's time duration and yields intersymbol interference (ISI). Frequency

selectivity and ISI are major inhibitors of mobile communications. Several mitigation techniques exist, and will be discussed in Section 2.5.4.

2.1.4.2 Flat Fading

Frequency non-selective fading or flat fading occurs when

$$\sigma_\tau \ll T_s \quad (2.8)$$

and

$$B_c \gg B_s \quad (2.9)$$

In this case, all the received multi-path components of a symbol arrive within the symbol time duration so that the components are not resolvable. Flat fading channels are also referred to as narrowband channels, since the bandwidth of the transmitted signal is narrow as compared to the channel coherence bandwidth. Because the signal time spreading does not result in significant overlap among neighbouring symbols, there is no channel induced ISI distortion. Performance is still degraded by deep fades however, since the unresolvable phasor components can add up destructively. Loss of SNR due to flat fading can be addressed by introducing some form of signal diversity and through the use of error-correction coding.

2.1.5 Fading effects due to Doppler spread

Delay spread and coherence bandwidth are parameters which describe the small-scale time dispersive nature of the channel. The parameters Doppler spread B_d and coherence time $(\Delta t)_c$ are used to analyse the time varying nature of the channel that is caused by either relative motion between the mobile and the base station, or by movement of objects within the channel. A vehicle driving past buildings, for example, will cause the channel conditions for a cellular call in progress to fluctuate and the rate of this fluctuation depends on the relative velocity of the surrounding environment. Doppler spread is a measure of the spectral broadening caused by the time rate of change of the mobile radio channel and is defined as the range of frequencies over which the received Doppler spectrum is non-zero. The amount of spectral broadening depends on the Doppler shift, expressed as [5]

$$f_d = \frac{v}{\lambda} \cos \theta \quad (2.10)$$

where v is the relative velocity of the mobile, λ is the wavelength of the carrier wave, and the θ is the angle between the direction of motion of the mobile and the direction of arrival of the multi-path signals.

2.1.6 Coherence Time

Coherence time $(\Delta t)_c$ is the time domain dual of Doppler spread and is the time duration over which two received signals have a strong potential for amplitude correlation. A practical relationship between the two parameters is [2]

$$(\Delta t)_c = \sqrt{\frac{9}{16\pi f_m^2}} \quad (2.11)$$

where f_m is the maximum Doppler shift given when $\theta = 0$. A channel can be classified as a fast fading or slow fading channel depending on how rapidly the transmitted baseband signal changes as compared to the rate of change of the channel.

2.1.6.1 Fast Fading

For fast fading the channel impulse response changes rapidly within the symbol duration. That is, the coherence time of the channel is smaller than the symbol period of the transmitted signal which leads to signal distortion. For this reason fast fading is sometimes referred to as time selective fading. Viewed in the frequency domain, an increase in Doppler spread relative to the bandwidth of the transmitted signal causes an increase in fast fading and subsequently signal distortion. For fast fading

$$T_s > (\Delta t)_c \quad (2.12)$$

and

$$B_s < B_d \quad (2.13)$$

In practice, fast fading only occurs for very low data rates [2].

2.1.6.2 Slow Fading

In the slow fading case the impulse response of the channel varies more slowly than the transmitted signal and can therefore be considered to remain static over one or more symbol periods. Looking at this case in the frequency domain, we can say that the Doppler spread of the channel is much less than the bandwidth of the baseband signal; therefore, a signal undergoes slow fading if

$$T_s \ll (\Delta t)_c \quad (2.14)$$

and

$$B_s \gg B_d \quad (2.15)$$

Clearly, it is the relative velocity of the mobile user and the baseband signal duration that indicates whether a transmitted signal will undergo fast or slow fading.

2.2 The Cellular Concept

2.2.1 Early Systems

Early mobile radio systems were designed to achieve a large coverage area by mounting a single high powered antenna on a tall tower. This provides broad coverage, but what happens when all the available frequencies are used? Since any attempt to reuse the same frequencies within the system will result in interference, any new calls placed will be blocked until someone else completes a call. This problem could be solved by allocating more frequency spectrum for mobile services; however, spectrum was a scarce resource and it soon became obvious that a new system design was required.

2.2.2 Frequency Reuse

The cellular concept offered high capacity with a limited spectrum allocation without major technology changes. A cellular network replaces a single high power transmitter (large cell) with many low power transmitters (small cells), each providing a fraction of the total coverage area. Each base station is provided with a portion of the total number of frequency bands or channels available in such a manner that cells adjacent to one another do not share the same group of channels and thus interference between base stations (and mobile users)

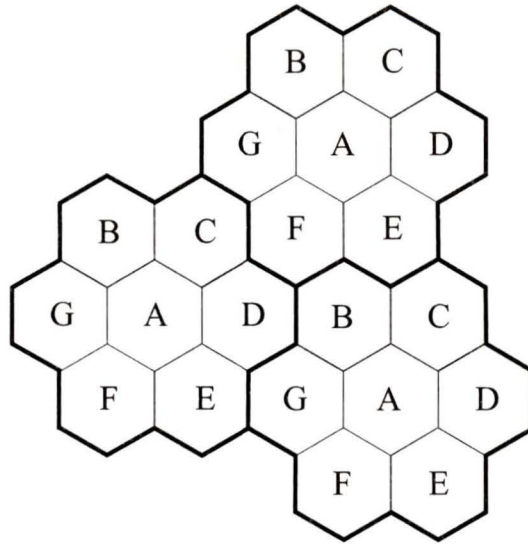


Figure 2.1. *Illustration of the cellular frequency reuse concept. Cells with the same letter use the same set of frequencies. The bold line encloses a cell cluster which is replicated over the service coverage area.*

is minimized. Figure 2.1 illustrates the concept of frequency reuse, where cells labeled with the same letter use the same group of channels. By systematically placing base stations throughout a market area, the available channels can be reused *ad infinitum*. When the number of subscribers exceeds the capacity of the cellular network the number of base stations may be increased while the transmitted power of each is decreased to avoid added interference. This method of providing additional capacity with no additional increase in radio spectrum is the fundamental principle on which all modern wireless communication systems are based.

2.2.3 Interference

As alluded to above, interference is the major limiting factor in the performance of cellular radio systems. Interference can be attributed to another mobile in the same cell, a call

in progress in a neighbouring cell, or other base stations operating in the same frequency band. The effects of interference include cross-talk on voice channels, lost user data, and missed or blocked calls due to errors in digital signaling. There are two major types of system generated interference - co-channel and adjacent channel interference. Co-channel interference is a result of frequency reuse. Cells using the same set of frequencies are called co-channel cells, and the interference between signals from these cells is called *co-channel interference*. Interference resulting from signals which are adjacent in frequency to the desired signal is called *adjacent channel interference*. Adjacent channel interference results from imperfect receiver filters which allow nearby frequencies to leak into the passband. The two types of interference are generally termed multiple access interference (MAI). As the name implies their effects depend on the multiple access scheme implemented. MAI is difficult to control due to the random propagation effects of the environment.

2.3 Ways To Improve Capacity

A reduction in cell size will increase cellular system capacity. This cell size reduction can be accomplished using cell splitting and sectoring techniques [6], each of which can provide significant increase in capacity. The minimum cell size allowable is determined by taking into account (1) the minimum co-channel reuse distance that can be achieved while maintaining a minimum quality of service; (2) the problem of siting the base stations; and (3) the costs involved in increasing the number of cells. Consider the effect of cutting the radius of each cell in Figure 2.1 in half. In order to cover the entire service area with smaller cells, approximately four times as many cells would be required with a corresponding increase in cell overhead costs. When the minimum cell size is reached new methods must be used to increase capacity. In addition, next generation wireless networks will provide users with new services and much higher data rates. With these new data rates it is conceivable that a single user may require the entire bandwidth available in a single cell in today's cell networks. Thus, cell size reduction alone is not sufficient to provide increased capacity.

Another possibility for improving capacity is to obtain additional bandwidth (radio channels). In 1989 the FCC granted an additional 10 MHz (166 channels) to U.S. cellular service providers to accommodate the rapid growth in demand. Allocating new frequency spectrum allows present multiple access schemes and medium access protocol to be maintained while providing a dramatic increase in capacity. Radio spectrum however, is a scarce resource that is coveted by its owners and difficult to redistribute. While new spectrum may

become available it is always prudent to make the most of what you have before requesting more.

Making the most of radio spectrum means developing an efficient means of sharing the available bandwidth among users. This sharing is achieved through a multiple access scheme which is designed to maximize (with given constraints) bandwidth efficiency (bits/second/Hz). Improving the multiple access scheme increases cell capacity without the need for additional spectrum or reducing cell dimensions and provides the motivation for this thesis. The development of future cellular networks hinges on improved spectral efficiency to enable the higher bit rates that users demand. Current cellular systems manage a mere 0.2 bits/s/Hz while wireline modems operating on a 3kHz telephone line are reaching 128 bits/s for a spectral efficiency of 42 bits/s/Hz. While the wireless channel is a far inferior medium for communication there certainly remains room for improvement. In this thesis improvement in cellular capacity is sought through the investigation of the MC-CDMA scheme.

2.4 Multiple Access Schemes

There are basically three multiple access methods distinguished by the means (frequency, time, code) used in implementation:

- Frequency division multiple access (FDMA)
- Time division multiple access (TDMA)
- Code division multiple access (CDMA)

2.4.1 FDMA

Frequency Division Multiple Access assigns individual channels to individual users for the duration of their call as illustrated in Figure 2.2. In a FDMA/FDD system a pair of channels is assigned for the downlink (mobile user to base station) and uplink (base station to user) where FDD stands for frequency division duplexing. The Analog Mobile Phone System (AMPS) uses FDMA/FDD.

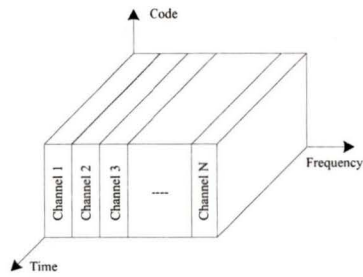


Figure 2.2. In FDMA different channels are assigned to different frequencies. Guard intervals are inserted between.

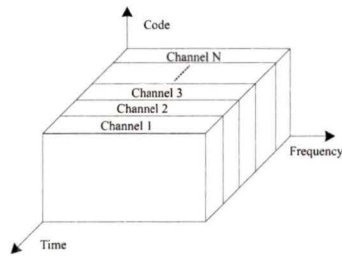


Figure 2.3. In TDMA a channel occupies a time slot within a repetitive time frame. Guard times are required between time slots to minimize ISI.

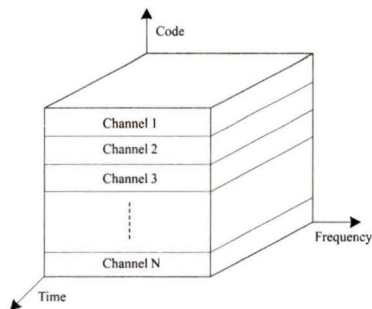


Figure 2.4. In CDMA each channel is assigned a unique PN code which is orthogonal to other users PN codes.

2.4.2 TDMA

The requirement for increased capacity sparked development in TDMA systems, where the Nyquist sampling theorem is applied to accommodate an increased data rate per channel. Subsequently, a channel can be shared by several users, each of which can use the channel for a fixed non-overlapping time period. TDMA (Figure 2.3) systems transmit data by buffer-and-burst, thus transmissions are non-continuous. Thus, unlike FDMA systems which allow analog frequency modulation, digital data and digital modulation must be used. IS-54 developed in the late 1980's is a cellular standard which incorporates TDMA into AMPS by dividing each frequency channel into three to six time slots thus offering up to six times the capacity of AMPS as well as the extra services possible from a digital system [2]. Because IS-54 combines FDMA and TDMA techniques, it is referred to as a hybrid multiple access technique. Overall TDMA systems deliver increased spectral efficiency over analog systems [2].

2.4.3 CDMA

In code division multiple access systems (Figure 2.4) the users access the channel in a random manner using spread spectrum techniques to differentiate users. Hence, the signal transmissions among multiple users completely overlap in both time and frequency. The two major varieties of CDMA are direct sequence CDMA (DS-SS) and frequency hopping CDMA (FH-SS) [7]. Introduced to the commercial cellular world with Qualcomm's IS-95 standard proposal, DS-SS has been the subject of intense research. Initial claims of multiple access capacity improvements almost an order of magnitude over TDMA [8] have since been reduced considerably, due to practical considerations most importantly being the requirement for strict power control between the base station and the mobile receiver. CDMA is still accepted to provide a modest increase over TDMA systems [2].

2.4.4 Narrowband and Wideband

Depending on how the spectrum is used, a multiple access scheme can be broadly classified as narrowband or wideband. Narrowband implies that the spectrum is split into several narrowband channels which are less than the coherence bandwidth of the propagation channel, whereas in a wideband scheme the whole (or a significant amount) of the band is available to all users. FDMA is intrinsically narrowband, while CDMA is wideband. TDMA, however,

can be implemented either as a narrowband or wideband system.

2.5 Hybrid Multiple Access Schemes

In recent years several new hybrid multiple access techniques have been proposed that combine the benefits of more than one multiple access scheme into a single scheme. Multi-Carrier Code Division Multiple Access (MC-CDMA), proposed in late 1993 [4, 9], is one such technique. MC-CDMA is based on a combination of DS-CDMA and Orthogonal Frequency Division Multiplexing (OFDM).

2.5.1 DS-CDMA

The advantages of spread spectrum are well known with the most important being: high immunity against multi-path distortion, no need for frequency planning, high flexibility, and easier (relative to FDMA and TDMA) variable rate transmission. DS-CDMA relies on spreading the data stream using a unique time domain spreading code for each user. To accomplish this the carrier is first modulated by the baseband digital information with rate $R_b = 1/T_b$, where T_b is the baseband signal duration. This modulated signal is in turn modulated by a pseudo-noise sequence (PN) that has a bit rate (chip rate) several orders of magnitude greater than the required bandwidth. This converts the narrowband signal to a wideband noise-like signal.

The cross-correlation properties of the spreading codes allow the multiple access interference (MAI) to be reduced. In a multi-path environment the ability to distinguish one component from others in the composite received signal is given by the auto-correlation properties of the spreading codes. A RAKE receiver takes advantage of this ability by using multiple correlators, each matched to a different resolvable path in the received composite signal, to obtain multiple independently faded copies of the transmitted signal. The term RAKE receiver stems from the fact that the correlators (called fingers) that form the RAKE receiver form a rake shape when viewed as a functional block diagram. The performance of a DS-CDMA system will depend heavily on the number of active users, the channel characteristics, and on the number of correlators (RAKE *fingers*) in the receiver. The capacity is limited by self- and multiple access interference (MAI), which results from imperfect auto- and cross-correlation properties of the codes after they have passed through the frequency selective channel. As the number of simultaneously active users increases,

the performance of DS-CDMA rapidly degrades. Another drawback of this system is its complexity. Exploiting all of the available multi-path diversity requires D arms, where $D_{max} = (\tau_{max}/(\Delta t)_c) + 1$ [10]. It is very difficult for a DS-CDMA system to use all of the received signal energy that is scattered in the time domain and hence, it is difficult to maximize capacity.

2.5.2 OFDM

The technique of multi-carrier transmission has also been receiving attention recently for the purposes of high data rate applications. Multicarrier modulation has been shown to be robust to frequency selective fading, have reduced signal complexity by equalization in the frequency domain, and have good narrowband interference rejection. Multi-carrier modulation (MCM) is based on transmitting high data rates by splitting the data into several low rate data streams and then using each sub-stream to modulate a separate orthogonal subcarrier. By using a large number of sub-carriers immunity against multi-path fading is provided. The symbol duration T_s of each sub-stream will be much greater than the channel time dispersion σ_τ , hence the effects of intersymbol interference (ISI) will be minimized.

Early MCM modulators used conventional FDM methods by separating the sub-carriers using filters. Due to difficulties in implementing sharp filters each signal used a bandwidth, $(1 + \alpha)f_s$, which was greater than the Nyquist minimum, f_s , thus achieving a bandwidth efficiency of $f_s/\delta f = 1/(1 + \alpha)$ [11]. In 1971 a technique termed orthogonal frequency division multiplexing (OFDM) [12] was developed where the sub-carriers were generated using Binary Phase Shift Keying (BPSK) modulated signals. The individual spectra become overlapping sinc functions, and, while not bandlimited they can still be separated by the receiver without the use of bandpass filtering. The means of separation, and the major advantage of this approach, is accomplished today through the use of discrete Fourier transforms (DFT). Today's semiconductor technology has allowed up to several thousand sub-carriers to be generated in this manner. Residual ISI in MCM can be completely suppressed if a guard interval larger than the channel time delay is inserted into each OFDM symbol [13].

OFDM has enjoyed many breakthroughs recently, being chosen for ADSL in the US [14], for the European digital audio broadcasting (DAB) standard [13, 14, 15], as well as for the European digital terrestrial television broadcasting (DTTB) system [16, 17].

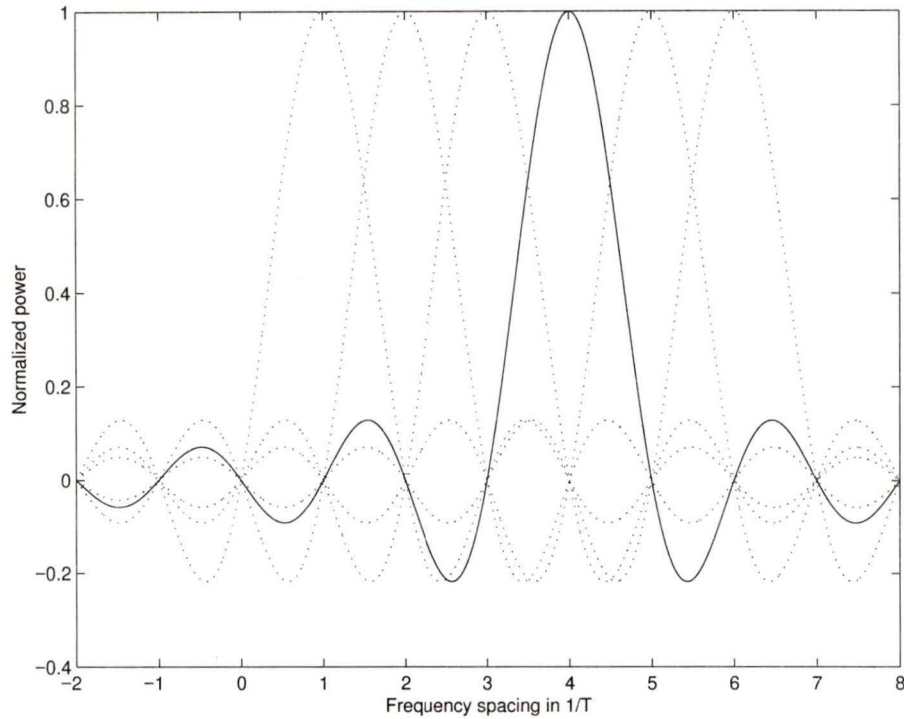


Figure 2.5. *Orthogonal spectra of OFDM signal.*

2.5.3 MC-CDMA

The advantages of OFDM, combined with the advantages of bandspreading, code division, and frequency diversity of DS-SS, prompted many researchers to investigate the suitability of a hybrid of MCM and spread spectrum, known as MC-SS. This hybrid technique, introduced as a multiple access scheme in late 1993, combines the advantages of both schemes to provide higher spectral efficiency, simpler detection techniques, and higher flexibility. It is particularly suited for the downlink where its unique structure allows for the low complexity and power efficiency that are essential in mobile receivers. Our investigation of MC-SS will focus on this suitability for the mobile radio downlink, beginning with a more thorough description of OFDM.

2.5.4 Principles of OFDM

In an OFDM system the total bandwidth B available for transmission is divided into N_c sub-bands with orthogonal subcarriers, spaced by B/N_c . The input bit sequence with a high rate R is multiplexed into N_c parallel sequences with data rate $R_s = R/N_c$. Each sequence

modulates one of N_c subcarriers leading to a narrowband signal. The transmitted power spectra of the sub-bands of an OFDM system form mutually overlapping sinc functions that exactly meet the Nyquist criteria for distortionless transmission, therefore giving optimum bandwidth efficiency, as shown in Figure 2.5. However, due to the multi-path fading of the mobile radio channel, the condition of perfect orthogonality (no ISI) between subcarriers is lost. For this reason, a guard interval T_g is added to each symbol before transmission. If the guard interval T_g is greater than the delay spread σ_τ then the channel can be considered flat fading for each subcarrier. Furthermore, if the symbol time $T_s = N_c T_b$ is much smaller than the coherence time $((\Delta t)_c \gg T_s)$ then the channel is constant over several MC-CDMA symbols. Each sub-carrier will therefore experience slow flat-fading channel conditions, which is the ideal case for a mobile transmission channel. Over the entire bandwidth B the independently faded subcarriers result in high frequency diversity. However, in order to exploit this diversity and improve the performance, this system should be combined with coding [18].

The frequency f_n for the n -th subcarrier is $f_n = f_0 + \frac{n}{T_s}$ where $n = 0, 1, \dots, N_c - 1$ or, using the notation that will be used throughout this thesis $n = 0 : N_c - 1$, and f_0 is the lowest frequency. The guard interval T_g is a periodical extension of the signal as seen in Figure 2.6. Delayed signal copies resulting from multi-path propagation are absorbed by the guard interval. The effective symbol interval then becomes $T_s = T'_s + T_g$. The OFDM basis functions are defined by

$$\phi_k(t) = \begin{cases} e^{j2\pi f_k t} & \text{if } T_g \geq t < T_s \\ 0 & \text{otherwise} \end{cases} \quad (2.16)$$

This definition accounts for the periodic extension of the OFDM symbol into the guard interval. The inclusion of the guard interval implies that a small amount of transmitted power is ignored in the receiver. As well, the guard interval causes a small degradation in spectral efficiency [13]. The transmitted OFDM baseband signal $x(t)$ has a non-constant envelope and is the sum of N_c parallel subcarrier signals,

$$s(t) = \sum_{n=-\infty}^{+\infty} \sum_{k=0}^{N_c-1} s_{n,k} \phi_k(t - nT) \quad (2.17)$$

where $s_{n,k}$ are the modulated symbols transmitted on the k th subcarrier in the n th OFDM symbol. From Equations 2.16 and 2.17 we can see that $s(t)$ can be obtained by performing an inverse Fourier transform. Both the inphase and quadrature phase components of $s(t)$

need to be transmitted since the values of $s_{n,k}$ are asymmetrical in the frequency domain.

Given an ideal noise-free channel the transmitted signal $s(t)$ can ideally be restored at the receiver using a Fourier transform [18]

$$\begin{aligned}
 Y_{n,k} &= \frac{1}{T_s} \int_{nT}^{nT+T_s} s(t) \phi_k^*(t - nT) dt \\
 &= \frac{1}{T_s} \int_{nT}^{nT+T_s} s(t) e^{-j2\pi f_k(t-nT)} dt \\
 &= s_{n,k}
 \end{aligned} \tag{2.18}$$

The Fourier transform acts as a filter matched to the basis function $\phi_k(t)$ $0 \leq t \leq T_s$, without cyclic extension, of each subcarrier k , $k = 0 : N_c - 1$.

Let us consider the transmission of a single OFDM signal over the multi-path channel. The channel can be modelled using an impulse response $h(t)$. Since the OFDM signal consists of narrowband flat fading subcarriers, $h(t)$ can be represented in the frequency domain as a series of discrete coefficients $h_{n,k}$ representing the complex response at subcarrier f_k for time nT . For a single OFDM symbol Equation 2.17 can be written as

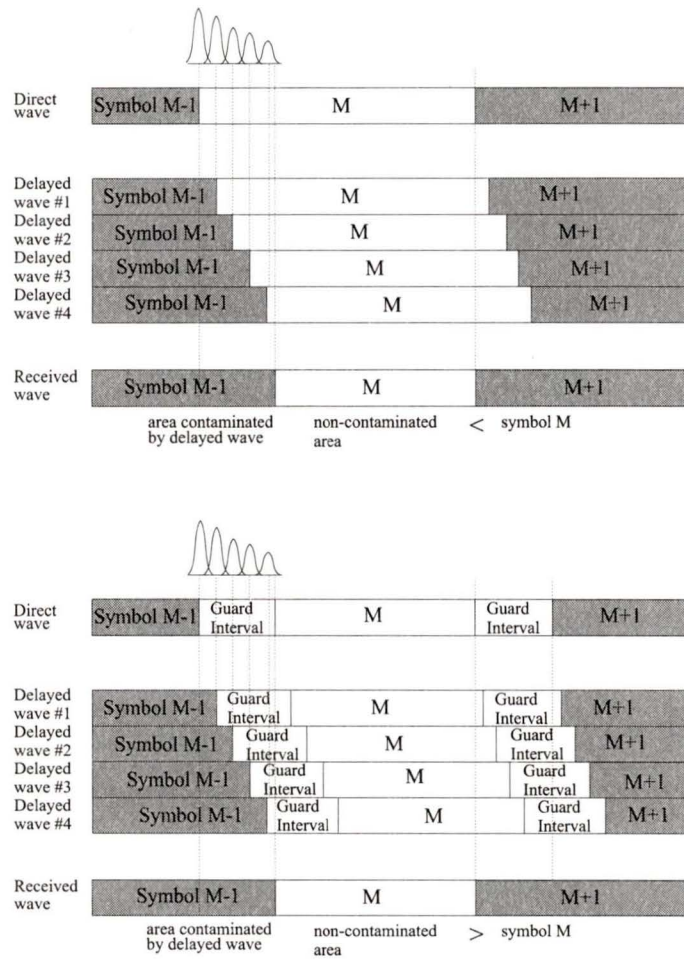


Figure 2.6. Illustration of the cyclical extension of the MC-CDMA symbol to form the guard interval.

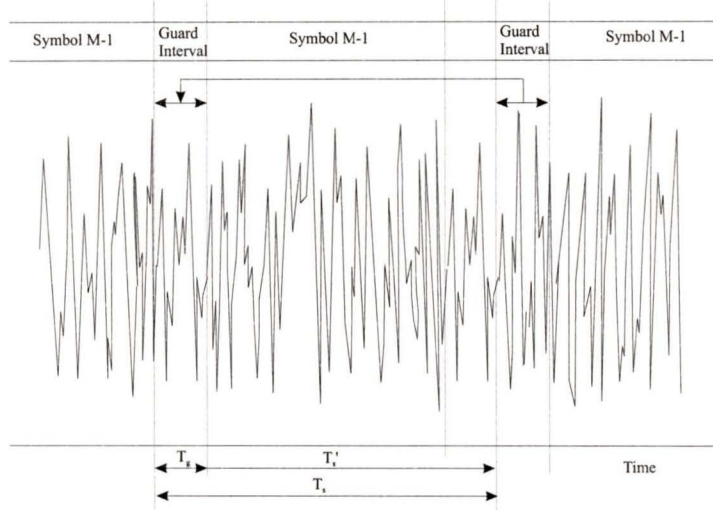


Figure 2.7. *The effect of guard interval insertion.*

$$s_n(t) = \sum_{k=0}^{N_c-1} s_{n,k} e^{j2\pi f_k t} \quad 0 \leq t < T_s \quad (2.19)$$

For time instance nT , the received signal then becomes

$$y_n(t) = \sum_{k=0}^{N_c-1} h_{n,k} s_{n,k} \phi_k(t - nT) \quad 0 \leq t < T_s \quad (2.20)$$

and the output of the decoder is given by

$$h_{n,k} s_{n,k} = \frac{1}{T_s} \int_{-\infty}^{\infty} y_n(t) \phi_{n,k}^*(t) dt \quad (2.21)$$

Thus, from Equation 2.21 and as emphasized in Figure 2.7, all ISI has been removed by the guard interval. The effects of the remaining flat fading of the subcarriers can be addressed by using channel sounding techniques to obtain estimates for $h_{n,k}$. These estimates however, can only be determined on the downlink since on this link the transmitted signal originates from one source (ie. the base station) and therefore encounters one set of channel conditions. The uplink link consists of many geographically distributed mobile units, all of which will experience different channel fading conditions and thus single values of $h_{n,k}$ will not exist.

Localised low signal-to-noise ratios will still be encountered in OFDM due to imperfect channel estimations. To combat deep fades coding can be introduced, as implemented in coded OFDM. The performance of C-OFDM is degraded by the adverse effects of a high peak to mean power ratio (crest factor) [19]. An alternative to C-OFDM is to use DS-CDMA techniques to add redundancy to the OFDM scheme, referred to as Multi-Carrier CDMA.

2.5.5 Advantages of MC-CDMA

2.5.5.1 Compared to Direct Sequence DS-CDMA

DS-CDMA is a method to share spectrum among multiple simultaneous users. Moreover, it can exploit frequency diversity by using RAKE receivers. However, in a dispersive multipath channel DS-CDMA with a spread factor N can accommodate N simultaneous users only if highly complex interference cancellation techniques are used. MC-CDMA can handle N simultaneous users with good BER, using standard receiver techniques.

2.5.5.2 Compared to C-OFDM

To avoid excessive bit errors on subcarriers that are in a deep fade, OFDM typically applies coding. Hence, the number of subcarriers needed is larger than the number of bits or symbols transmitted simultaneously. MC-CDMA replaces this encoder by an $N \times N$ matrix operation which results in an improved BER [4].

2.5.6 Definition of MC-CDMA

There are many equivalent ways to describe MC-CDMA:

1. MC-CDMA is a form of CDMA or spread spectrum, but the spreading is applied in the frequency domain rather than in the time domain as in Direct Sequence CDMA.
2. MC-CDMA is a form of Direct Sequence CDMA, but after spreading a Fourier Transform (FFT) is performed.
3. MC-CDMA is a form of Orthogonal Frequency Division Multiplexing (OFDM), but we first apply an orthogonal matrix operation to the user bits. Therefore, MC-CDMA is sometimes also called "CDMA-OFDM".

4. MC-CDMA is a form of Direct Sequence CDMA, but our code sequence is the Fourier Transform of a Walsh Hadamard sequence.
5. MC-CDMA is a form of frequency diversity. Each bit is transmitted simultaneously (in parallel) on many different subcarriers. Each subcarrier has a constant phase offset. The set of frequency offsets form a code to distinguish different users.

2.5.7 Implementation using FFT

The discrete Fourier transform (DFT) implementation of OFDM can be done simply and efficiently through the use of the fast Fourier transform (FFT) algorithm [12]. In a mobile receiver FFTs can be used to extract only the desired signal from the OFDM frame. This greatly simplifies the receiver structure.

2.6 The MC-CDMA signal

This section will describe the MC-CDMA signal structure. Following this general investigation, Chapter 3 will give a thorough description of the parameters used to evaluate the MC-CDMA system.

2.6.1 Spreading Codes

In order for the spreading codes to be orthogonal they must satisfy the relationship

$$\sum_{i=0}^{N-1} c_l^i c_m^i = N \delta_{l,m} \quad (2.22)$$

where c_l^i and c_m^i are the l and m elements codes for user i respectively. Shift register generated psuedo-random (pn-codes) are one possible code set that meets this condition. The codes are called psuedo-random because while they appear to be random, they are in fact deterministic, with an equal number of -1's and 1's. Using a shift register of length n , the generated codes will be of length $2^n - 1$. Since only odd length codes can be generated these codes are not perfectly orthogonal. Furthermore, if the transmitter is to be implemented with an FFT then the code lengths should be a multiple of 2, which pn-codes are not capable of generating.

Walsh-Hadamard (WH) codes are also orthogonal, and can be generated from the Walsh-Hadamard matrix of

$$C_0 = \begin{bmatrix} 1 & 1 \\ 1 & -1 \end{bmatrix} \quad (2.23)$$

Codes of length 2^n can be generated with the following recursive matrix operation

$$C_n = \begin{bmatrix} C_{n-1} & C_{n-1} \\ C_{n-1} & -C_{n-1} \end{bmatrix} \quad (2.24)$$

where the matrix C_n of size $2^n \times 2^n$ is formed using the matrix C_{n-1} of size $2^{n-1} \times 2^{n-1}$ with C_0 given in Equation 2.23. Each row of C_n gives the orthogonal code for one user. The cross correlation between any two different codes is zero, thus these codes are perfectly orthogonal. These codes will be used in this thesis, however, further investigation into coding is carried out in Chapter 4.

2.6.2 Transmission scheme

Figure 2.8 illustrates a simple MC-CDMA transmitter model for the i th user. The i th $i = 1 : N_u$ users data sequence is defined by

$$d^i(t) = \sum_{n=-\infty}^{\infty} d_n^i \cdot p_{T_b}(t - nT_b) \quad (2.25)$$

where $d_n^i \in \{1, -1\}$ and

$$p_{T_b}(t) = \begin{cases} 1 & \text{if } 0 \leq t \leq T_b \\ 0 & \text{otherwise} \end{cases} \quad (2.26)$$

If each of the N_u users sends K bits per MC-CDMA symbol then the data vector of user i is given by

$$d = [d_0^i, d_1^i, \dots, d_{K-1}^i]^T \quad (2.27)$$

where d_k^i is the k th bit of the i th user. In this analysis it is assumed the data values are equiprobable and that if user i is inactive then $d = 0$. Each bit d_k^i of user block i is spread by a WH spreading sequence

$$c_i(t) = \sum_{l=1}^L c_i(t) \cdot p_{T_c}(t - lT_c) \quad (2.28)$$

where L is the length of the codeword, T_c is the chip period and

$$p_{T_c}(t) = \begin{cases} 1 & \text{if } 0 \leq t \leq T_c \\ 0 & \text{otherwise} \end{cases} \quad (2.29)$$

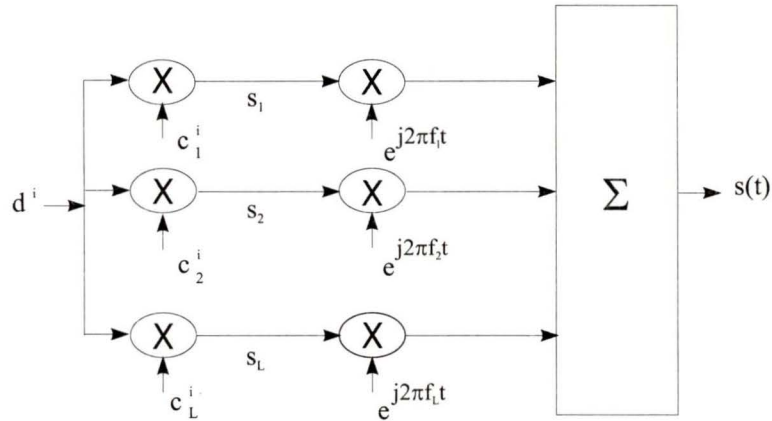


Figure 2.8. Model of an MC-CDMA transmitter.

The code elements $[1, -1]$ equate to encoding the user data, and subsequently, the narrowband subcarriers with phase offsets of $[0, \pi]$ when binary phase-shift keying (BPSK) is applied. The WH code matrix can be defined as

$$C = \begin{bmatrix} c_0^0 & c_1^0 & \cdots & c_{L-1}^0 \\ c_0^1 & c_1^1 & \cdots & c_{L-1}^1 \\ \vdots & \vdots & \ddots & \vdots \\ c_0^{L-1} & \cdots & \cdots & c_{L-1}^{L-1} \end{bmatrix} \quad (2.30)$$

where the i th row vector c^i corresponds to the spreading code c_l^i , $l = 0 : L - 1$ of the i th user. This system will generate $N_c = K \times L$ subcarriers where subcarrier n , $n = 1 : N_c$ transmits the sum of N_u bit synchronized chips. In the sequel, transmission of a single data bit d_k^i is considered, which for brevity is denoted by d^i . Using this notation, the data

modulated spreading sequences of all users are added chip-synchronously and the sum can be written as the vector \vec{S} in Figure 2.8

$$\vec{S} = [s_1 \ s_2 \ \cdots \ s_L]^T \quad (2.31)$$

and

$$s_l = \sum_{i=1}^{N_u} d^i c^i. \quad (2.32)$$

After serial-to-parallel conversion the components of \vec{S} are interpreted as complex frequency values of the $N_c = L$ subcarriers. The values S_l are real valued in this case since BPSK is applied. Other modulation schemes can be used as well, generally resulting in complex valued components of \vec{S} . The continuous-time transmitted signal for the MC-CDMA system is obtained by an inverse DFT followed by parallel-to-serial conversion and appropriate low pass filtering, and can be stated as

$$s(t) = \sum_{l=1}^{N_c} s_l e^{j2\pi f_l t} \quad (2.33)$$

where $f_l = f_0 + \frac{l-1}{T_s}$ is the subcarrier carrier frequency and $t \in [0, T_s]$. The addition of a guard interval T_g is required to avoid intersymbol interference. This addition causes

$$s(t), t \in [0, T_s] \rightarrow s(t), t \in [-T_g, T_s] \quad (2.34)$$

If no channel distortion is present the data for the i th user can be recovered using the orthogonality of the codes;

$$d^i = \frac{1}{N_u} c^i \vec{S} \quad (2.35)$$

where \cdot denotes the inner product of two vectors and T denotes the transpose of vector \vec{S} .

The MC-CDMA receiver for user i is shown in Figure 2.9. The received signal is sampled and the inverse OFDM operation is performed. The inverse OFDM operation is represented in this model by N_c matched filters with one matched to each subcarrier. Each matched filter consists of an oscillator with a frequency corresponding to the frequency of the particular BPSK modulated subcarrier of interest and an integrator. In addition, a phase offset equal to the phase distortion is included in the oscillator for synchronization in time. To

extract the desired signal component the corresponding chip from the desired user's code is multiplied with it. Each signal component is multiplied by an equalization gain factor g_l which is based on the estimates of \mathbf{H} .

The received signal vector \vec{R} for a single user (ie. no multiple access interference) can be written as

$$\vec{R} = \mathbf{H}\vec{S} + \vec{N} \quad (2.36)$$

where \mathbf{H} is the $N_c \times N_c$ diagonal channel matrix with diagonal elements h_n , $n = 1 : N_c$ and \vec{N} is a vector of N_c complex additive white Gaussian noise (AWGN) samples. The elements of h_n are the discrete values of the channel transfer function $H(f)$ at the corresponding subcarrier frequencies f_n , $h_n = h(f_n)$ and can be referred to as the channel coefficients.

For downlink MC-CDMA transmissions, the focus of this thesis, the mobile terminal receives interfering signals designated for other users ($i = 1 : N_u$) through the same channel as the desired signal ($i = 0$). The aim is to design the signal structure such that the delay spread σ_τ is much smaller than the symbol period T_s and the coherence time $(\Delta t)_c$ is much greater than the symbol period. The effect of the channel on the i th subcarrier, therefore, can be approximated by a constant amplitude scaling ρ_i and a constant phase offset θ_i over the symbol duration. The channel transfer function for the continuous-time fading channel for all transmissions to user $i = 0$ can be represented by

$$h\left(f_0 + \frac{n}{T_s}\right) = \rho_n e^{j\theta_n} \quad (2.37)$$

where the random amplitude ρ_n and phase θ_n of the channel at frequency $f_0 + n/T_s$ are independent of i . The phase shifts θ introduced by the channel are assumed to be independently and identically distributed (iid) random variables on the interval of $[-\pi, \pi]$ for all subcarriers.

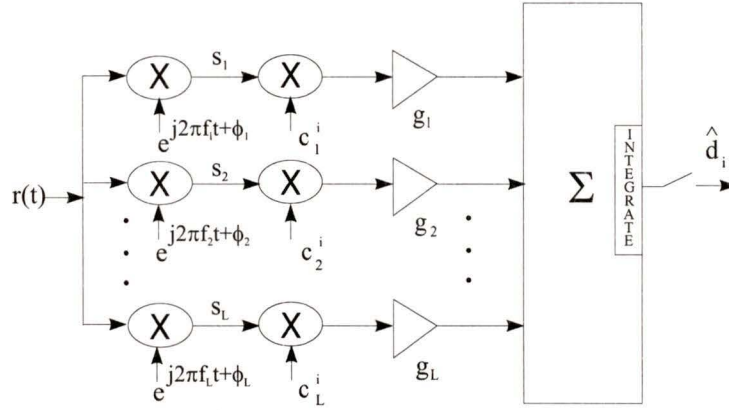


Figure 2.9. Model of an MC-CDMA receiver.

By employing channel estimation techniques, such as pilot tone calibration, we can assume perfect phase correction. Following this assumption the channel matrix \mathbf{H} is given by

$$\mathbf{H} = \begin{bmatrix} h_1 & 0 & \cdots & 0 \\ 0 & h_1 & \cdots & 0 \\ \vdots & \vdots & \ddots & \vdots \\ 0 & \cdots & \cdots & h_{N_c} \end{bmatrix} \quad (2.38)$$

Detection strategies for this received signal will be discussed in detail in Chapter 4.

2.7 Advantages of MC-CDMA

2.7.1 Flexible data rates

The combination of DS-CDMA and OFDM provides MC-CDMA with many advantages over other schemes. The use of multiple subcarriers provides an extra degree of freedom over DS-CDMA. At maximum data rate $N_c = KL$ subcarriers are used. If a lower rate will suffice then $k \times L$, $k < K$ subcarriers can be sent. Alternatively, if a higher data rate is required then user groups can be introduced to provide even more flexibility (Section 3.6.2).

2.7.2 Reduced multiple access interference

The orthogonality of the spreading codes minimizes multiple access interference (MAI). This MAI is independent of spreading code length thus allowing for low processing gains, where high data rates can be achieved using narrow system bandwidth.

2.7.3 Multipath Fading Mitigation

The most familiar approach to reducing the effects of multi-path fading is to perform time domain equalizations. Time domain equalization involves the use of filtering to restore the original waveform [10]. In a CDMA system, an elegant equalization procedure can be used which offers the possibility of collecting energy from different paths. Using a Rake receiver [20], the wide bandwidth of a frequency selective channel is resolved into uncorrelated multi-path components. In this manner, a multi-path gain over narrowband signaling can be obtained. Another approach is to perform equalization in the frequency domain. In order to accomplish this, the time domain signal must first be converted to the frequency domain where equalization is performed, and subsequently converted back to the time domain for demodulation [21]. MC-CDMA can benefit from frequency equalization in that the multi-carrier signal is already in the frequency domain. Thus, a simplified form of frequency equalization can be performed.

2.7.4 Frequency diversity

By spreading every user bit and sending the resulting chips on separate subcarriers frequency diversity is achieved. Frequency interleaving of the subcarriers (Section 3.5.1) improves this diversity. The extra diversity can be exploited through various detection strategies, as discussed in Section 4.1. Having described MC-CDMA in some detail, the next chapter will provide a formulation of the parameters used to simulate the MC-CDMA system.

Chapter 3

MC-CDMA System Definition

The MC-CDMA system parameters must be selected according to the requirements discussed in Chapter 2. For example, the subcarrier bandwidth chosen must satisfy Equations 2.8 and 2.9 in order for the assumption of a flat fading channel to be valid. Tables 3.1 and 3.2 in Section 3.8 summarize the values of the MC-CDMA system parameters determined in this chapter. With system specification complete an investigation of detection schemes can be carried out.

3.1 System Bandwidth

We begin by assuming an available transmission bandwidth of B . A bandwidth choice of 1.25 MHz will ensure compatibility to current systems. Due to the flexible nature of MC-CDMA, future bandwidths such as the 5 MHz bandwidth proposed for UMTS 2000 can be accommodated by simple scaling of system parameters.

3.1.1 Symbol Duration

For the purposes of spreading user bits, Walsh Hadamard spreading codes of length L are employed. Assume initially that a single bit per user is sent during each symbol duration T'_s . In a single carrier system (eg. DS-SS) the symbol period would be $T_s = 1/B = 0.8\mu\text{s}$, however, in MC-CDMA the bandwidth is divided into N_c subcarriers thus spreading the symbol duration to $T'_s = N_c/B$ (μs).

3.1.2 Processing Gain

The processing gain G_p of the MC-CDMA system is defined as the transmission bandwidth B divided by the bit rate R_b yielding

$$G_p = \frac{B}{R_b} = \frac{T_b}{T_c} = L \quad (3.1)$$

The processing gain gives a measure of the level of protection a users data receives against interference from other users.

3.2 Guard Interval

In order to reject the remaining intersymbol interference a guard interval T_g is placed between symbols. The guard interval is achieved by periodical extension of the MC-CDMA symbol such that $s(t)$, $t \in [0, T'_s] \rightarrow s(t)$, $t \in [-T_g, T'_s]$. The addition of the guard interval results in a small loss of detection energy. This loss is minimized by utilizing a large number of subcarriers. If each user generates K bits per MC-CDMA symbol, then $N_c = KL$ subcarriers are required to send each symbol. This results in an increased symbol duration. Increasing the symbol duration has the effect of reducing the loss of detection energy by decreasing the relative size of the guard interval. The maximum K will be limited by the coherence time $(\Delta t)_c$ of the channel so that the condition of slow fading is maintained.

3.3 Bad Urban Radio Channel

The channel model used to represent the mobile radio channel was developed by the COST project [22]. We have chosen the *bad urban* model for the following reason. The most important objective in designing a cellular network is to maximize capacity. The environment where any wireless network will be required to provide maximum capacity is the urban area; where most users will be concentrated during peak hours. The urban channel model is optimistic in the sense that its delay spread is shorter than that of the suburban model. Shown in Figure 3.1, the coefficients of the power delay profile represent the average instantaneous power delay profile measurements over a local area of a typical bad urban environment. This particular profile is often used for practical GSM simulations. It is interesting to note that the first two coefficients (ie. $0.0 \mu\text{s}$ and $0.2 \mu\text{s}$) are lower than expected. A typical

receiver will require time to acquire a *lock* on the transmitted signal due to synchronization, equalization, or power control requirements. The effect of this is simulated by reducing the mean power of the first two received multipath components.

3.3.1 Channel Parameters

The maximum excess delay is $\tau_{max} = 10 \mu s$ and the rms delay spread $\sigma_\tau = 2.486 \mu s$. The coherence bandwidth is calculated to be approximately 225 kHz. The coherence bandwidth is determined by a more complex method than described in Section 2.1.4. We consider the time-correlation function, as calculated from the delay power spectrum by Fourier transform, which gives the correlation value between amplitudes (and phases) at a given time difference. The coherence bandwidth is defined by the time difference where the normalized time-correlation function is reduced from 1 to a value of 0.5 (50 percent correlation). The carrier frequency f_c is chosen to be 1.2 GHz to reflect the current focus of standards research. Assuming a maximum mobile user velocity of $v = 120 \text{ km/hr}$ we can determine the maximum Doppler shift to be $f_m = v/\lambda = 133 \text{ Hz}$ and thus the coherence time of the channel (Δt_c) $\approx 3.2 \text{ ms}$. A guard interval of $T_g = 12 \mu s$ is chosen to combat the echoes of the channel. The total symbol duration then becomes $T_s = T'_s + T_g$.

3.4 Number of Subcarriers

In order to take advantage of the use of the FFT for OFDM modulation the number of subcarriers N_c is limited to powers of 2. We choose $N_c = 512$ resulting in a subcarrier spacing $\Delta f = B/N_c = 2.441 \text{ kHz}$ and a MC-CDMA symbol duration of $T_s = T'_s + T_g = 409.6 \mu s + 12 \mu s = 421.6 \mu s$. These choices assure slow flat fading. Thus, each subcarrier $n = 1 : N_c$, is influenced by a complex-valued Gaussian distributed channel coefficient h_n and the received signal magnitude $|R_n|$ is Rayleigh distributed.

3.5 Frequency Diversity

The Rayleigh fading experienced by all subcarriers in this transmission scheme is closely related to the problem of transmitting over D independent and identical Rayleigh fading channels [10]. By sending each user bit over L subcarriers a maximum diversity of $D_{max} = L$ can be achieved. The Rayleigh fading of different subcarriers is not statistically independent

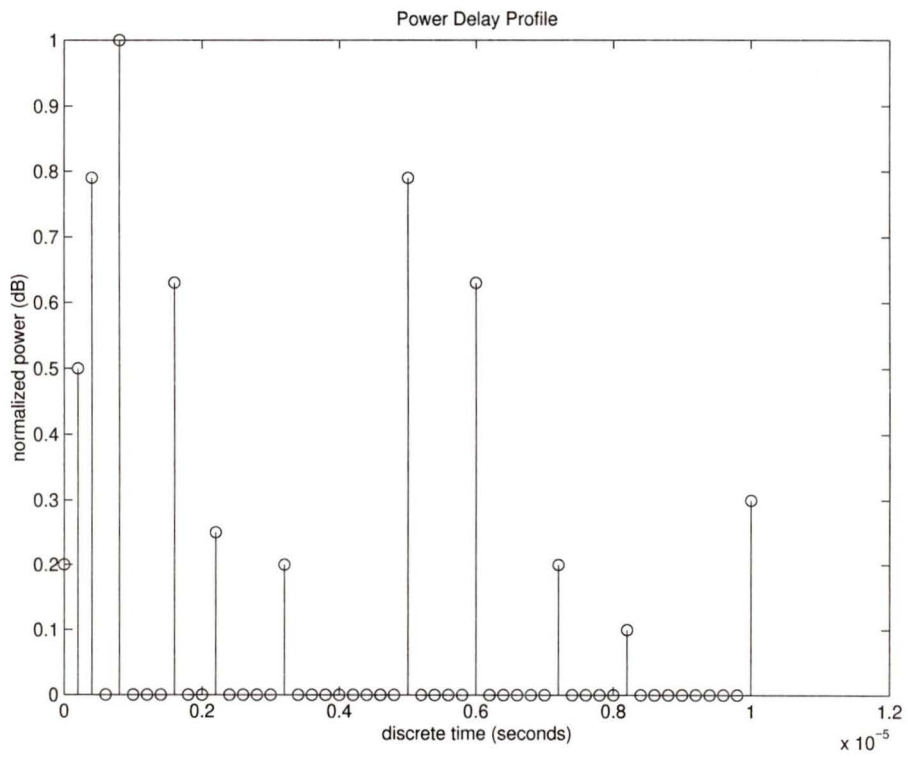


Figure 3.1. Instantaneous power delay profile for a COST bad urban channel.

and therefore the attainable diversity may be less than the number of chips $L = N_c/M$ of a single bit.

The achievable diversity is dependant on the channel and the transmission bandwidth which means that increasing L will not necessarily lead to increasing the available diversity. A rough estimation of diversity is given in [10]

$$D \approx B/(\Delta f)_c, \quad (3.2)$$

which results in $D \approx 5.5$ when applied to a typical bad urban channel.

The real achievable diversity for a MC-CDMA transmission scheme can be determined through simulations with various processing gains $G_p = L$ [23], since the number of subcarriers is fixed to $N_c = K \times L = 512$. As the processing gains vary the number of bits per MC-CDMA user block will vary as well.

3.5.1 Frequency Interleaving

As completely independent fading subcarriers cannot be assumed, frequency interleaving of the signal is introduced in order to reduce the correlation between the chips of a single bit. By reducing this correlation, an attempt is made to ensure that each chip of a single bit will experience different fading conditions thereby reducing the likelihood that several chips will experience deep fading. Frequency interleaving maintains the maximum available frequency diversity by separating the L chips in a bit by the maximum frequency spacing the system will allow. The frequency interleaving applied can be realized as a block interleaver with the L chips, $l = 1 : L$ of each bit k , $k = 1 : K$ are transmitted using subcarriers spaced equally at frequencies

$$f_{k,l} = \frac{[(k-1) + (l-1)K]}{T_s} \quad (3.3)$$

which gives a chip spacing of $(\Delta f)_{chip} = B/L = 156$ kHz between the L subcarriers carrying the chips of one bit. The correlation between two subcarriers separated by $(\Delta f)_{chip}$ is [5]

$$\rho((\Delta f)_{chip}) = \frac{1}{1 + (2\pi(\Delta f)_{chip})^2 \sigma_\tau^2} \quad (3.4)$$

With $(\Delta f)_{chip} = 156$ kHz the corresponding correlation is, $\rho((\Delta f)_{chip}) = 0.14$ when $\sigma_\tau = 2.4859 \mu s$.

If inter-cell interference is also considered, a psuedo-random frequency interleaving technique using frequency hopping can be employed [24]. In this thesis the MC-CDMA system is evaluated over a single cell only, thus only block interleaving is considered.

3.5.2 Achievable Diversity

Figure 3.2 shows the simulated bit error rate (BER) P_b versus the signal-to-noise ratio (SNR) E_b/N_0 for $L = 1, 2, 4, 8, 16, 32$ where E_b denotes the energy per transmitted bit and N_0 is the one-sided noise spectral density of the additive white Gaussian noise (AWGN). Since only a single active user is assumed then no multiple access interference exists. For the single user case the optimal detection scheme is maximal ratio combining (MRC) (Section 4.1.2.2) and is used for this simulation. To illustrate the diversity limits of the mobile radio channel we have included the theoretical curves for transmitting over $D = 1, 2, 4, 7, 8$ independent and identical (iid) Rayleigh fading channels. The simulation results are slightly worse than the theoretical BER curves due to the loss of detection energy resulting from the addition of the guard interval. We can see in Figure 3.2 that as L increases, the increase in diversity steadily diminishes until the limit of the channel and transmission bandwidth is reached.

3.6 Spreading Code Length

Making use of the results of Section 3.5.2 we can select a shorter code length that takes advantage of most of the available diversity. The acheived diversity is about $D = L$ for $L \leq 4$, since the L chips of a bit are independently Rayleigh faded. For $L \geq 8$ the frequency spacing is insufficiently large thus some statistical dependence is introduced implying that $D < L$. The maximum possible diversity for this transmission scenario is about $D_{max} = 8$ which can be nearly acheived using a processing gain of only $G_p = L = 8$.

3.6.1 Maximum Likelihood Detection

An advantage of selecting short spreading sequences is the possibility of using maximum likelihood detection (MLD). This method requires a search of all possible transmission patterns for the pattern most likely to have been sent. For BPSK transmission this implies a search of 2^L possible patterns. The use of MLD, while minimizing receiver complexity, makes short spreading sequences essential. MLD is investigated for our MC-CDMA system in Section 4.1.4.

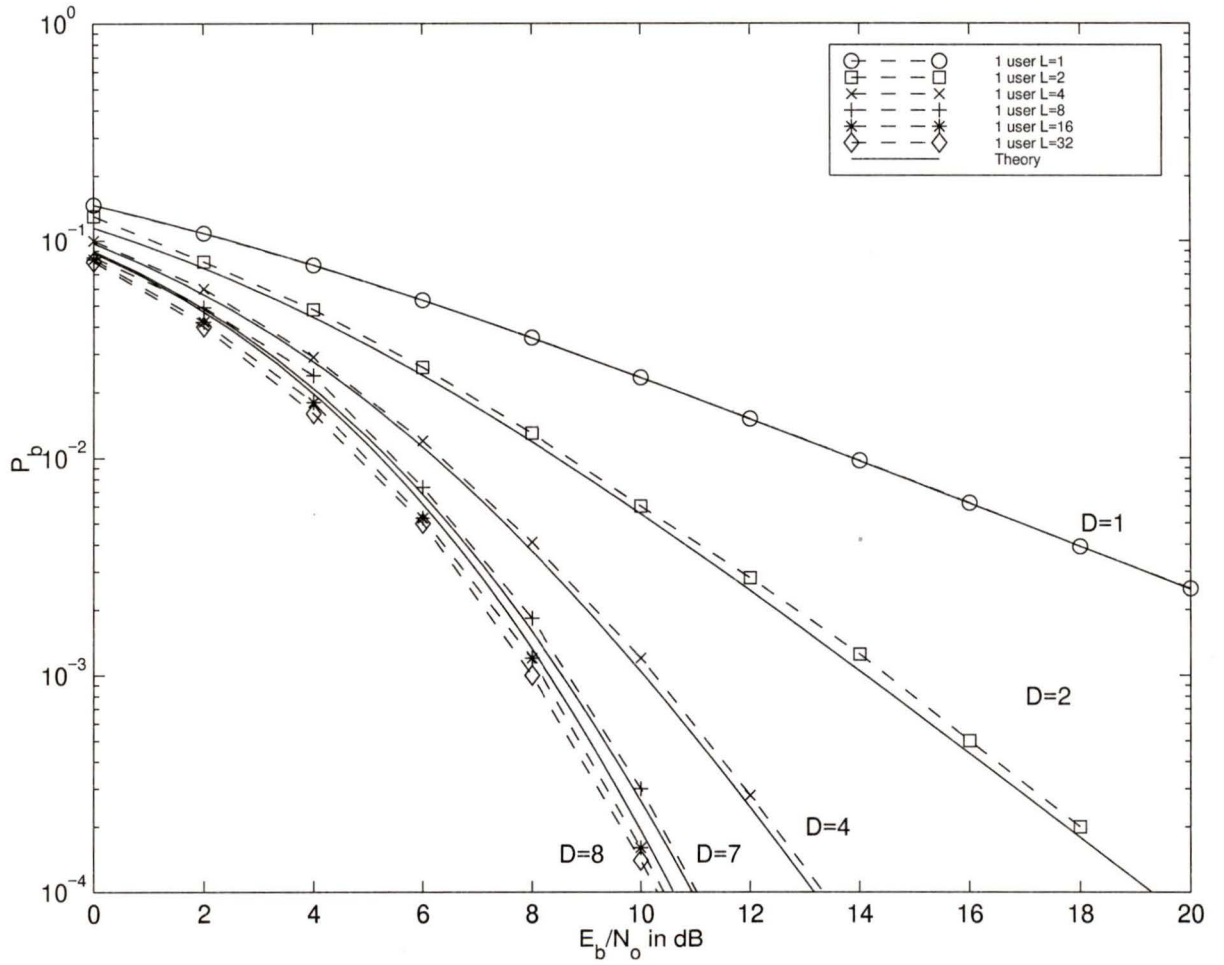


Figure 3.2. BER for single user case and different spreading code lengths $l = 1, 2, 4, 8, 16, 32$.

3.6.2 User Groups

The drawback of short spreading sequences is that they limit the number of users, since an $L \times L$ matrix can accommodate L users. To accommodate more users per cell the concept of user groups is introduced. If N_u users are grouped into Q user groups, each with N_u^q users, $q = 1 : Q$ then $N_c = Q \times K \times L$ subcarriers are generated by the MC-CDMA system. By fixing the spreading sequence length L the values of Q and K can be varied to exchange transmission rate $R_b = K/T_s$ for user capacity $N_u = Q \cdot L$ and *vice versa* with no loss in diversity. For example with $K = 8$ simultaneous bits per user then $N_u = L \cdot Q = 64$ active users can be accommodated with a bit rate of $R_b \approx 16$ *kbps*, allowing for a 15 % reduction in bit rate due to synchronization and channel sounding. Reducing K to 5 allows a bit rate of approximately 9.6 *kbps* which is a suitable rate for voice traffic while increasing the single cell capacity to 104 users. Conversely, a maximum bit rate of $R_b = 1.5$ *Mbps* can be achieved if the number of users in the cell is limited to $Q = 8$. These rates are presented assuming BPSK modulation, however they can be doubled if QPSK is employed.

Another benefit of introducing user groups to the MC-CDMA system is the reduction of mean MAI. This interference is confined to within user groups since only users within that group share the same subcarriers; therefore a scheme that evenly distributes users among user groups will minimize the number users in each group, and consequently minimize the MAI.

With $N_c = 512$, the values $Q = 8$ and $K = 8$ are chosen for system parameters. The modified frequency interleaver from Equation 3.3 that is required to take into account each user group q is

$$f_{q,k,l} = [(q - 1) + (k - 1)Q + (l - 1)KQ]/T_s \quad (3.5)$$

The spacing between subcarriers remains B/L , while the introduction of user groups can be viewed as the addition of an FDMA component. The deterministic frequency interleaver employed is shown in Figure 3.3.

The performance improvement obtained using interleaving is illustrated in Figure 3.4. By separating adjacent subcarriers as much as possible, their correlation is decreased thus improving the effective diversity of the system.

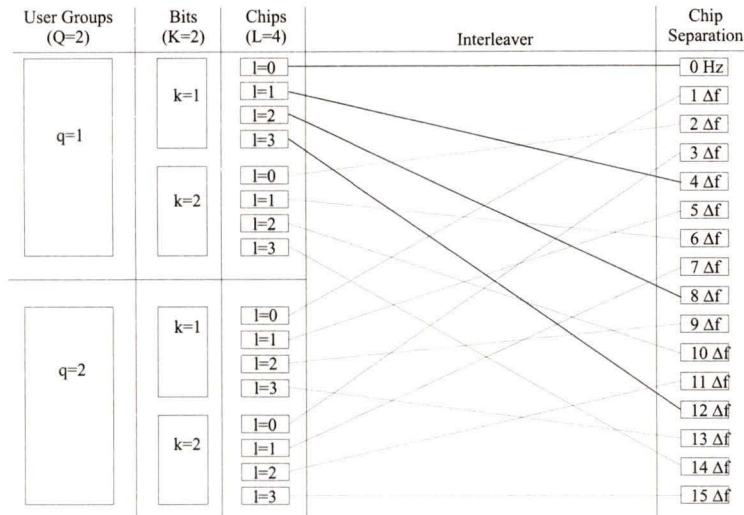


Figure 3.3. Illustration of the deterministic frequency interleaver employed with $Q=2$, $K=2$, and $L=4$.

3.7 Channel Sounding

Channel sounding is the term used to describe the means of obtaining estimates for the channel transfer function \mathbf{H} in Equation 2.38. One method of channel sounding is called pilot tone channel estimation. The basic principle of pilot tone channel estimation is to multiplex training symbols known to the receiver into the data stream. The receiver is then able to use observations at the pilot locations to interpolate the channel estimates with any time-frequency index, assuming the sampling rate is sufficient with respect to the channel bandwidth [25]. Sounding intervals are spaced as far apart in time as possible so as to make the resulting loss in data throughput negligible. Pilot tone channel estimation in the time domain or frequency domain alone is well understood. Many different 1-D interpolation filters have been investigated. For multi-carrier modulation techniques such as OFDM applications, two dimensional channel estimation is useful for multi-carrier modulation techniques such as OFDM applications since the redundancy as well as the estimation error can be reduced compared to scattering the pilot tones in only one domain [26, 27].

By choosing $T_s < (\Delta t)_c$, the channel will remain relatively constant over a symbol duration. Successive symbol durations will be assumed to encounter different channel conditions; therefore, channel sounding will need to be performed periodically based on the time rate

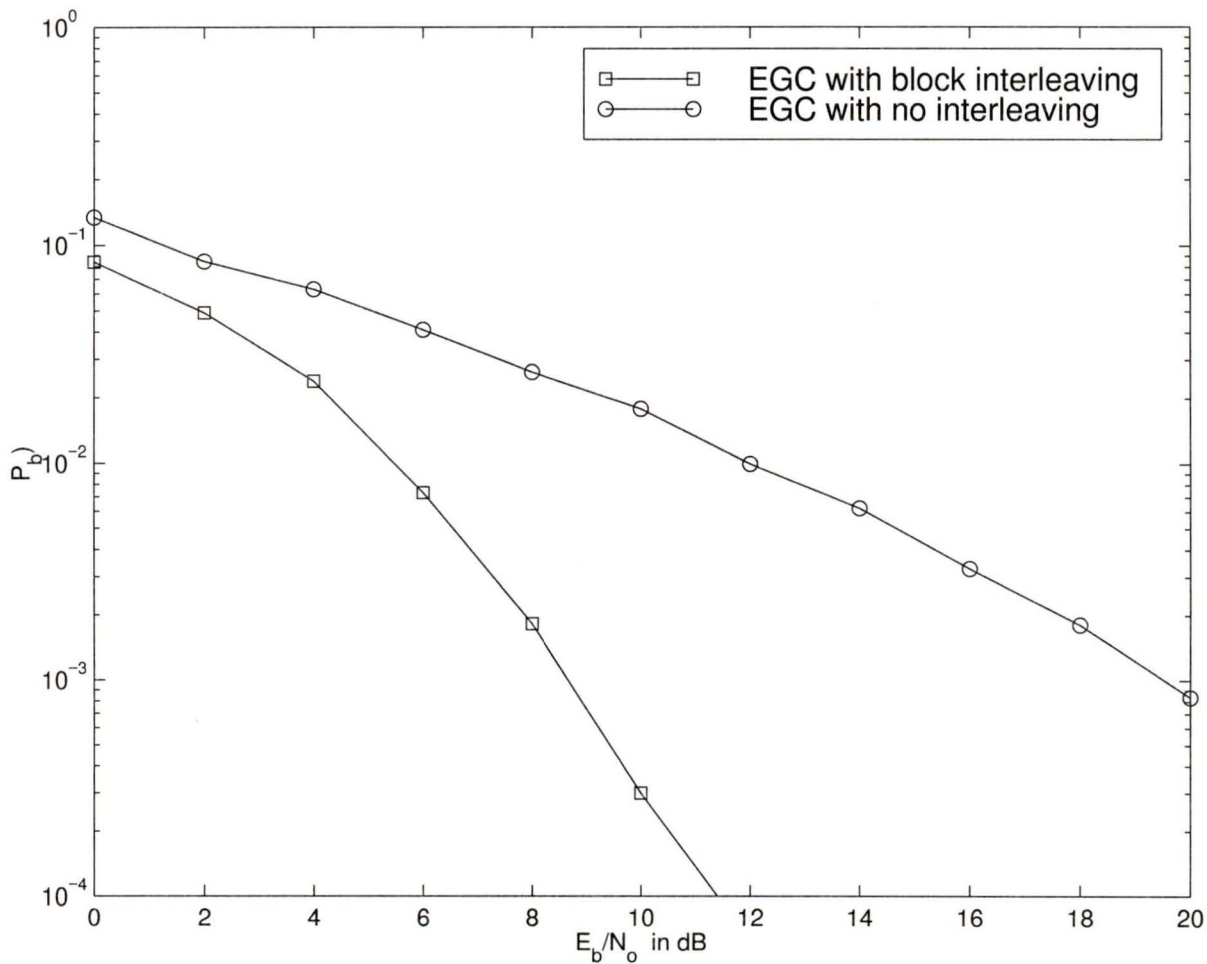


Figure 3.4. Performance improvement resulting from increased frequency diversity through block interleaving.

of change of the channel in order to minimize the channel estimation error. Additionally, we can use the statistical dependence that exists between adjacent subcarriers in order to place the pilot-symbols as far apart as possible in the frequency domain. The dependence between adjacent subcarriers was shown in Figure 3.4 where the superior performance of the interleaved subcarriers is attributable to decreased dependence between adjacent subcarriers and thus increased diversity.

3.7.1 Grid Design

The object of this section is to determine a time invariant sampling grid design for our system. A method for designing a two dimensional channel estimation grid for mobile radio application is presented in [28]. We denote the spacing between pilot symbols in the time domain by N_k and in the frequency domain by N_L . Given the normalized channel bandwidths $f_D T_s$ and $\tau_{max} \Delta f$, the sampling theorem requires that

$$f_d T_s N_k \leq 1/2 \quad (3.6)$$

and

$$\tau_{max} \Delta f N_L \leq 1/2 \quad (3.7)$$

A balanced design is defined as having

$$f_d T_s \cdot N_k \approx \tau_{max} \Delta f \cdot N_L \quad (3.8)$$

The balanced design is optimal if the Doppler power spectrum and the power delay spectrum have the same shape, as can shown by symmetry considerations. Reasonable filter complexity (latency) can be achieved using $2\times$ oversampling, resulting in

$$f_d T_s N_k \approx 1/4 \quad (3.9)$$

and

$$\tau_{max} \Delta f N_L \approx 1/4 \quad (3.10)$$

Given our system constraints a grid design with $2\times$ oversampling is determined as follows:

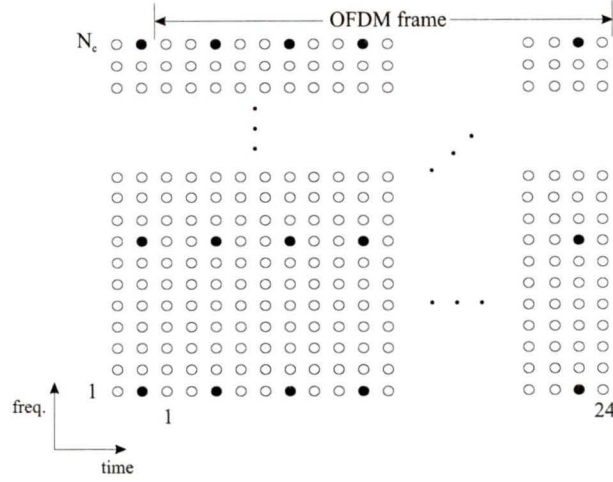


Figure 3.5. MC-CDMA frame with 512 subcarriers showing pilot tone placement with $N_l = 10$ and $N_k = 4$.

$$f_d T_s N_k = 133\text{Hz} \times 421.6\mu\text{s} \times 3 \approx 1/4 \quad (3.11)$$

$$\tau_{max} \Delta f N_L = 10\mu\text{s} \times 2.441\text{kHz} \times 7 \approx 1/4 \quad (3.12)$$

By sampling the channel every third symbol in the time domain and every seventh subcarrier in the frequency domain, accurate channel coefficients $H_{l,k}$ can be obtained. The pilot tone density produced by this method is

$$1/N_k N_l = 1/21 \quad (3.13)$$

Balanced designs for the diagonal grids have also been considered [26], where it was found that the diagonal and rectangular grids had similar performance. An illustration of our 2-D grid design is provided in Figure 3.5. For our system a frame size consisting of 24 MC-CDMA symbols was selected for the purposes of channel sounding.

The subcarriers designated for channel sounding should be assigned values from a pseudo-noise sequence in order to minimize the peak to mean power ratio of the MC-CDMA symbol. Part of the sequence is repeated if the number of pilot tones in one MC-CDMA symbol, $N_p \neq 2^i - 1$, where $i > 1$. In general, a random sequence in the frequency domain

will be transformed into a random sequence in the time domain, thereby minimizing the crest factor (see Section 4.4).

3.8 System Parameters

Table 3.1 presents the channel parameters assumptions, followed by Table 3.2 which provides system parameters chosen to evaluate the MC-CDMA system.

The overall system configuration is presented in Figure 3.6 for a base station and a mobile user within that base station's coverage area. As previously mentioned, the MC-CDMA structure lends itself to simple digital signal processor (DSP) techniques. Performing the OFDM operation using FFT operations as well as equalization in the frequency domain greatly facilitate simple DSP implementation.

Table 3.1. Channel parameters assumptions

Parameter	Symbol	Value
rms delay spread	σ_τ	2.486 μs
maximum excess delay	τ_{max}	10 μs
coherence bandwidth (@ 1.2 GHz)	B_c	255 kHz
coherence time	$(\Delta t)_c$	3.2 ms
maximum user velocity	v	120km/hr
maximum Doppler frequency	f_d	133 Hz

Table 3.2. System parameters

Parameter	Symbol	Value
carrier frequency	f_c	1.2 GHz
system bandwidth	B	1.25 MHz
number of subcarriers	N_c	512
subcarrier bandwidth	Δf	2.441 kHz
spreading code length	L	8
max. number of bits per symbol	K	8
number of user groups	Q	8
max. number of users per user group	L	8
pilot tone density	p	1/40
pilot tone frequency spacing	N_l	4
pilot tone symbol spacing	N_k	10
chip diversity spacing	$(\Delta f)_{chip}$	156 kHz
chip correlation	$\rho((\Delta f)_{chip})$	0.14
symbol duration	T_s	421.6 μ s
guard time	T_g	12 μ s
maximum capacity	N_u	64
user bit rate	R_b	190 <i>kbps</i>
maximum user bit rate	R_{max}	1.52 MHz

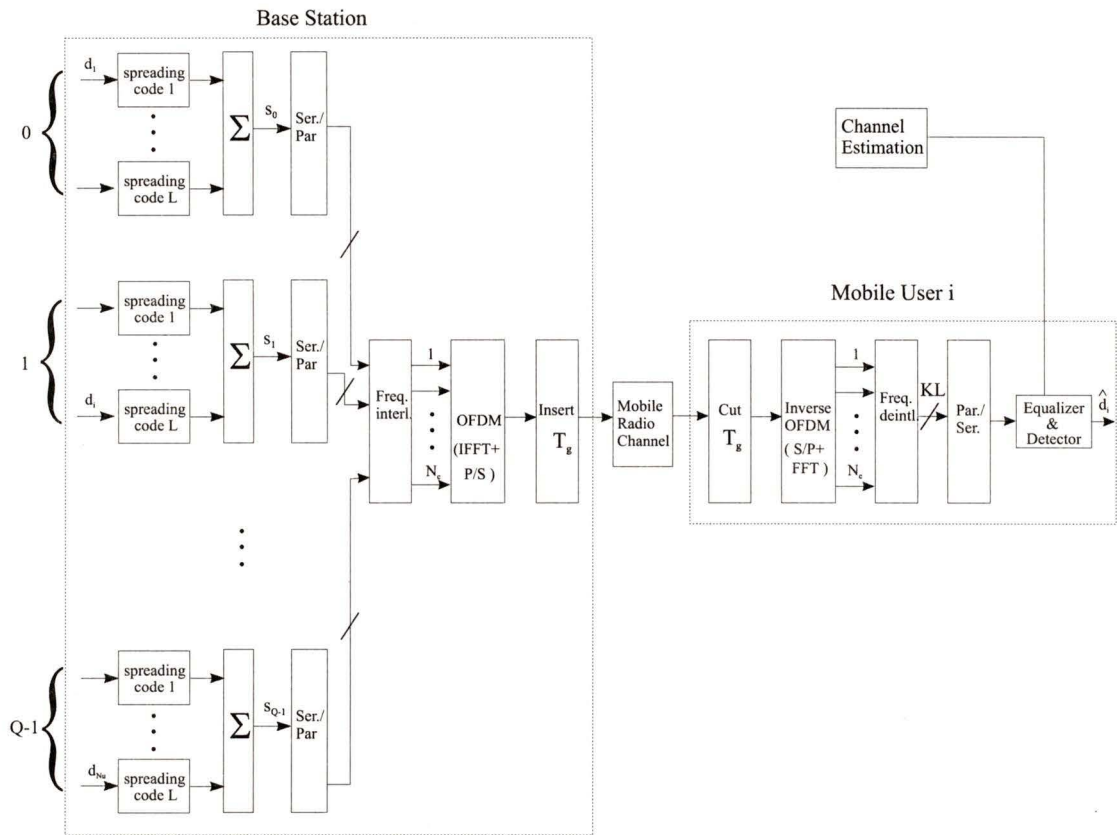


Figure 3.6. The overall system configuration for the base station and the mobile user.

Chapter 4

Design Considerations

In this chapter some important aspects of the design of a MC-CDMA system are considered. The first section examines the performance of detection techniques with varying degrees of complexity. The simulation results are presented and discussed. Following this channel coding is added to the simulation as would be the case in most implementations of MC-CDMA. Another important topic is the selection of spreading codes for the system; this topic is investigated with respect to receiver complexity, crest factor, and fading performance. Finally, a general approach to crest factor reduction is outlined and performance results from simulation are presented.

4.1 Detection Schemes

Now that the MC-CDMA system has been defined, an investigation will follow into the performance of various detection schemes. The underlying goal of these techniques should be to reduce the effect of fading and the multiple access interference (MAI) while not enhancing the effect of noise. The term equalization is most often used to describe the time domain process of removing the effects of ISI on the received signal. Since the guard interval in our system is chosen longer than the channel's delay spread, all the echoes are absorbed within the guard interval. Therefore, the received signal is free of ISI and there is no need for time domain equalization. Equalization is required in frequency domain. Frequency domain equalization in an OFDM based system refers to the process of restoring the effects of the channel on the amplitude and phase of the received subcarriers. Thus equalization in this context will refer to frequency equalization. After equalization and de-spreading of the received vector, the decision is made using the resulting bit estimate. To evaluate the merits of each equalization scheme it is assumed that perfect channel estimations are available as well as perfect bit synchronization.

The conventional detection schemes considered are inverse gain combining (INV), equal gain combining (EGC), maximum ratio combining (MRC), and minimum mean square error (MMSE). These schemes are sometimes called orthogonality restoration combining (ORC) [4] techniques since by compensating for the channel fading they have the effect of restoring the orthogonality of the received signal. As well, controlled equalization (CE) techniques are employed where the gain factor used on each subcarrier depends on the amount of fading it experiences. Multi-user detection (MUD) is examined next. This technique is used to perform interference cancellation (IC) on the received signal. The contributions of all interfering users are evaluated and then used to remove the effect of MAI on the desired signal. The use of reliability information is considered in the final case. In this method soft decisions are made on unreliable information in an attempt to reduce error propagation in IC systems. Lastly, we evaluate the use of maximum likelihood detection (MLD).

It is assumed in the following that the phase shift of all subcarriers is corrected, noting that if phase shift is not restored then the BER is 0.5.

The received signal $r(t)$ of Figure 2.9 can be written as the vector \vec{R} after OFDM demodulation and de-interleaving with

$$\vec{R} = \mathbf{H}\vec{S} + \vec{N} \quad (4.1)$$

as in Equation 2.36. In matrix form this is written:

$$\begin{pmatrix} r_1 \\ r_2 \\ \cdots \\ r_L \end{pmatrix} = \begin{pmatrix} h_1 & 0 & \cdots & 0 \\ 0 & h_2 & & \vdots \\ \vdots & & \ddots & \vdots \\ 0 & \cdots & \cdots & h_L \end{pmatrix} \begin{pmatrix} s_1 \\ s_2 \\ \vdots \\ s_L \end{pmatrix} + \begin{pmatrix} n_1 \\ n_2 \\ \vdots \\ n_L \end{pmatrix}. \quad (4.2)$$

The system is designed to have $T_g > \tau_{max}$, therefore there is no ISI and the matrices H and G are diagonal. For brevity the diagonal components of H and G , $h_{l,l}$ and $g_{l,l}$ respectively are denoted by h_l and g_l . The complex conjugate operation is denoted by $(\cdot)^*$. To simplify notation, we assume that only a single bit $K = 1$ per user is transmitted simultaneously. \vec{R} consists of L components assigned to one data vector d where L is the length of the spreading code, and consequently the maximum number of users in each user group is also L . The $L \times L$ matrix \mathbf{H} describes the complex channel fading coefficients

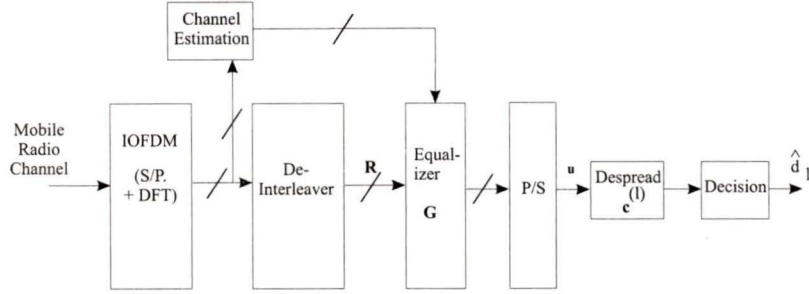


Figure 4.1. *The MC-CDMA receiver*

on the L subcarriers assigned to the transmitted vector \vec{S} . The vector \vec{N} represents the Gaussian noise. After equalization the received signal can be written as

$$u = \vec{G}\vec{R} = \vec{G}\mathbf{H}\vec{C}\vec{d} + \vec{G}\vec{N} \quad (4.3)$$

The $L \times L$ matrix G represents the complex equalization coefficients obtained from pilot tone aided channel estimation. After de-spreading and threshold detection we obtain the detected data vector. The detected data bit \hat{d}^l of user l corresponds to the sign of the scalar product of the received vector after equalization \vec{u} and the unique spreading code vector \vec{c}^l of user l as

$$\hat{d}^l = \text{sign}(\vec{u}, \vec{c}^l). \quad (4.4)$$

4.1.1 Orthogonality Restoration Combining

These methods make use of the channel estimates to repair the distortion caused by the channel. The block diagram of a MC-CDMA receiver using ORC equalization is shown in Figure 4.1 where the equalization gain coefficients are determined from the channel estimates.

4.1.2 Inverse Detection

The goal of inverse equalization is to normalize the channel transfer function using the inverse of the channel coefficient estimates. The equalization coefficients are

$$g_l = h_l^* , \quad l = 1 : L \quad (4.5)$$

In a noiseless environment inverse filtering ensures that the effect of the channel is completely removed assuming perfect channel estimation since

$$u_l = s_l + n_l \frac{h_l^*}{|h_l|^2}. \quad (4.6)$$

The above equation for the detected data bit indicates that inverse equalization suffers from noise enhancement due to division by h_l and thus will be effective only in high SNR environments.

4.1.2.1 Equal Gain Combining

Equal Gain Combining (EGC) can be used to restore the orthogonality of the received vector before de-spreading occurs; however noise amplification is again experienced. The equalization coefficients applied are

$$g_l = \frac{h_l^*}{|h_l|} , \quad l = 1 : L \quad (4.7)$$

The received signal resulting from EGC is given by

$$u_l = s_l |h_l| + n_l \frac{h_l^*}{|h_l|} \quad (4.8)$$

4.1.2.2 Maximum Ratio Combining

Maximum Ratio Combining (MRC) makes use of the relative amplitude information of the received signal \vec{R} . The subcarriers with larger amplitudes are assumed to have less noise corruption and therefore to have higher reliability. By squaring the amplitudes of the received vector, larger amplitudes will have more influence on the decision process. The equalization coefficients are

$$g_l = h_l^*, \quad l = 1 : L \quad (4.9)$$

The detector output after MRC is

$$u_l = s_l |h_l|^2 + n_l h_l^* \quad (4.10)$$

where it is evident that, while emphasizing strong amplitudes is good for the single user case, the increased loss in orthogonality will result in increased multiple access interference (MAI) in the multiuser environment.

4.1.2.3 Controlled Equalization

While EGC may be desirable for its simplicity and MRC for its noise combating capability, neither of these techniques make direct attempts to reduce the interference caused by other users. As our goal is to maximize capacity the channel model will change from a noise limited channel to an interference limited channel as the number of simultaneous users increases. Controlled equalization attempts to restore the orthogonality of the users by normalizing the amplitudes of the subcarriers. The equalization coefficients for CE depend on the amplitude of the subcarrier. A threshold value h_{thresh} can be chosen based on the SNR of the channel,

$$h_{thresh} = \sqrt{\frac{\rho}{SNR}} \quad (4.11)$$

where the SNR is determined from channel estimation and the scalar ρ can be optimized for the bad urban channel profile selected. Simulation results show a good choice for ρ is 0.4. Subcarriers whose amplitudes are below the threshold are ignored in the equalization process. For subcarrier amplitudes above h_{thresh} inverse equalization is employed due to its superior performance in high SNR environments. The equalization coefficients then are given as

$$|s_l| = \begin{cases} > h_{thresh} & \rightarrow g_l = \frac{1}{h_l} \\ < h_{thresh} & \rightarrow g_l = 0 \end{cases} \quad (4.12)$$

4.1.2.4 Minimum Mean Squared Error (MMSE) Equalization

MMSE equalization [10] minimizes the mean square value of the error ε_l between the transmitted signal s_l and the assigned output of the equalizer u_l on subcarrier l ,

$$\varepsilon_l = s_l - u_l, \quad l = 1 : L \quad (4.13)$$

The mean squared error $E\{|\varepsilon_l|^2\}$ is minimized when

$$\frac{d|\varepsilon_l|^2}{d|g_l|} = 0 \quad (4.14)$$

Using Equation 4.13 and Equation 4.14 the MMSE equalization coefficients for this MC-CDMA applications are [29]

$$g_l = \frac{h_l^*}{|h_l|^2 + \frac{LN_0}{2N_u E_b}}. \quad (4.15)$$

The second term of the denominator of Equation 4.15 acts as an adaptive threshold for equalization which depends on the SNR and the number of users N_u . Note that as the noise power N_0 approaches 0 then the equalization gain approaches that of inverse ORC. The output of the equalizer before de-spreading can be expressed as

$$u_l = s_l |h_l|^2 + \frac{n_{l,r} h_r + n_{l,i} h_i}{|h|^2 + \frac{LN_0}{N_u E_b}} \quad (4.16)$$

where $n_{l,r}$ and $n_{l,i}$ are the real and imaginary components of the noise acting on subcarrier l respectively.

4.1.3 Interference Cancellation through Multi-User Detection

The purpose of multi-user detection in the downlink of a mobile radio system is to remove the interference caused by users other than the desired user. This method requires the mobile receiver to know the spreading codes of all users. In performing interference cancellation the received vector for all $L - 1$ interfering users $l' = 1 : L$ with $l' \neq l$ are first detected using some form of equalization. Referring to Figure 4.2 the estimates for the received data bits of each user are \hat{d}^l , $l = 2 : L$. These estimates are re-spread by their corresponding spreading code to generate the vectors s_l , $l = 2 : L$. By making use of the results of channel sounding these vectors can be passed through the mobile radio channel again to

give $\hat{\vec{r}} = \mathbf{H}\vec{s}$. Subtracting these simulated received vectors from the original received vector reduces the interference caused by other users from the signal. If perfect channel estimation is assumed then the received signal vector after interference cancellation will carry no MAI and thus reduce to the single user case. Using EGC-ORC for final equalization will result in the equalizer output

$$u_l = (s_l - \hat{s}_l) |h_l| + n_l \frac{h_l^*}{|h_l|} \quad (4.17)$$

at the equalizer output. Two equalization schemes were investigated for the interference cancellation and the final detection. The schemes, denoted as MMSE-EGC MUD and MMSE-MMSE MUD were chosen based on bit error rate performance considerations. The notation of MMSE-EGC MUD implies that the interference cancellation was performed using EGC and the final equalization uses MMSE. The reasoning for the choice of equalization schemes will be addressed in the results section.

A problem encountered when using interference cancellation is error propagation. A bit incorrectly detected in $\hat{d}^l, l = 2 : L$ will result in poor interference cancellation on the received vector. A method of avoiding interference propagation is to introduce a soft decision whereby the reliability information about the detected bit is accounted for. With hard decision Equation 4.4 is employed to decide whether the despread received vector represents a transmitted 1 or -1 . Soft decision retains the original value of received vectors whose reliability falls below a certain threshold. Figure 4.3 presents the two possible filter shapes for retaining reliability information. The dotted lines of Figure 4.3 indicate the signal path for detection using soft interference cancellation.

4.1.4 Maximum Likelihood Detection (MLD)

In Section 3.6, modifications to the MC-CDMA transmission scheme were introduced in order to reduce the complexity of maximum likelihood sequence estimator (MLSE). Since the complexity of this technique grows exponentially when the number of users increases, the total number of users $N_u = 64$ is split into $Q = 8$ independent blocks or user groups. Hence, instead of 2^{64} possible transmitted sequences only $2^{64/8} = 256$ possible sequences need to be evaluated in the MLSE. The MLSE technique employed here assumes that there is no memory in the signals transmitted in successive symbol intervals. We wish to determine the signal s_n that minimizes the Euclidean distance

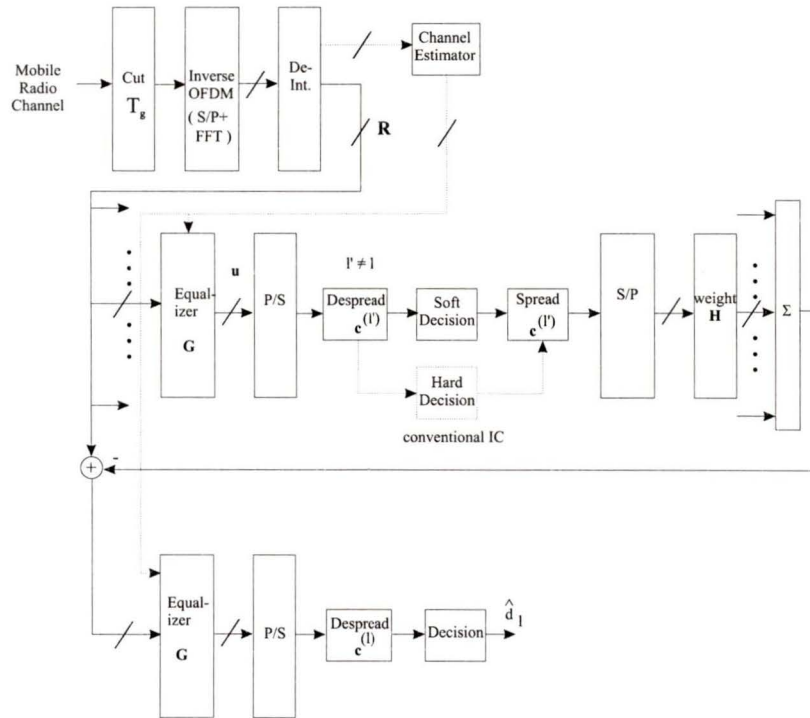


Figure 4.2. MC-CDMA receiver employing interference cancellation.

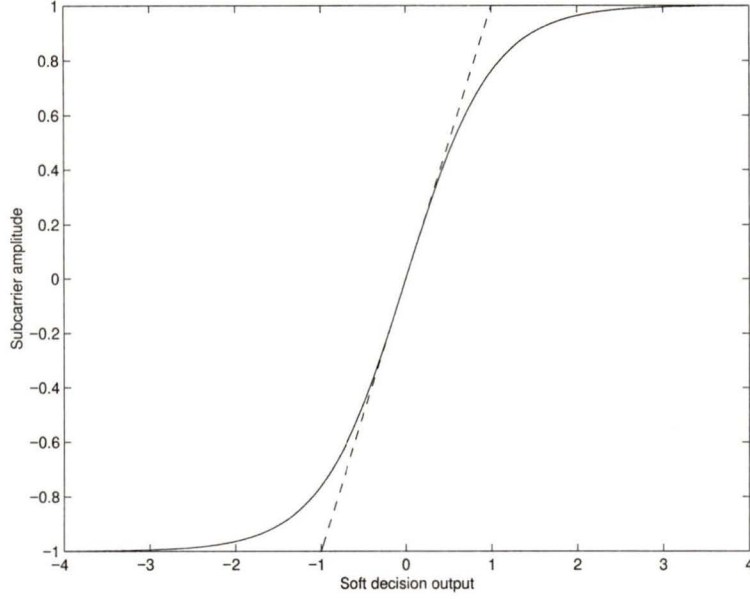


Figure 4.3. *Decision curves for soft decision detection.*

$$V(\vec{r}, \vec{s}_n) = \sqrt{\sum_{l=1}^L (r_l - s_{n,l})^2} \quad (4.18)$$

where $V(\vec{r}, \vec{s}_n)$, $m = 1 : 2^8$ are called the *distance metrics*. Hence, we wish to find the signal s_n that is the closest in Euclidean distance to the received signal vector \vec{r} .

4.2 Simulation Results

4.2.1 Orthogonal Restoration Combining

Results for INV, EGC, MRC, CE, and MMSE equalization are presented in Figures 4.4 to 4.8 for the Rayleigh fading channel described in Section 3.3. All results are obtained using Monte Carlo simulations. Each scheme is simulated for 1, 4 and 8 users per user group where 8 users/group corresponds to the maximum capacity of $N_u = 64$ users per cell. For the single user case there are in fact 8 users that can operate with no MAI due to the formation of user groups.

In Figure 4.4 it can be seen that using inverse equalization eliminates MAI, thus similar results are obtained for all traffic levels. The noise enhancement is detrimental to the effectiveness of this technique.

Figure 4.5 illustrates the effects of loss of orthogonality of the Walsh-Hadamard (WH) spreading codes as the number of users increases for EGC. At $N_u = 8$ it can be seen that a noise floor of approximately 18 dB exists for EGC.

In Figure 4.6 it can be seen that for the single user case (i.e in a noise limited channel) MRC performs well. This is expected since MRC is optimum where no MAI is present. However, as the number of users increases EGC has superior performance. To maximize the effectiveness of the codes it is desirable that the equalized subcarrier amplitudes be equal so that interference will be cancelled by the orthogonality of the codes. With MRC, the differences between amplitudes is increased due to the squaring operation, thus reducing orthogonality. For a low number of users, however, the channel remains noise limited and consequently, MRC performs better. Like INV and EGC equalization, MRC is of no practical use for the downlink when assuming full capacity and Rayleigh fading on the channel.

The simulation results for controlled equalization are given in Figure 4.7. Note that the optimum value for the threshold parameter ρ will vary with the given channel. It can be seen that the performance curves that controlled equalization outperforms both inverse and EGC equalization. This can be attributed to the ability of controlled equalization to suppress noise dominated subcarriers so that they do not affect the detection process. It can also be noted that CE gives similar performance regardless of the number of active users which can be attributed to the use of inverse equalization for subcarriers above the threshold.

MMSE equalization, shown in Figure 4.8, outperforms all previous techniques at full capacity. In this case the orthogonality of the WH codes is significantly restored in the receiver while high noise amplification is avoided by using a gain that is dependent on the number of users and the SNR.

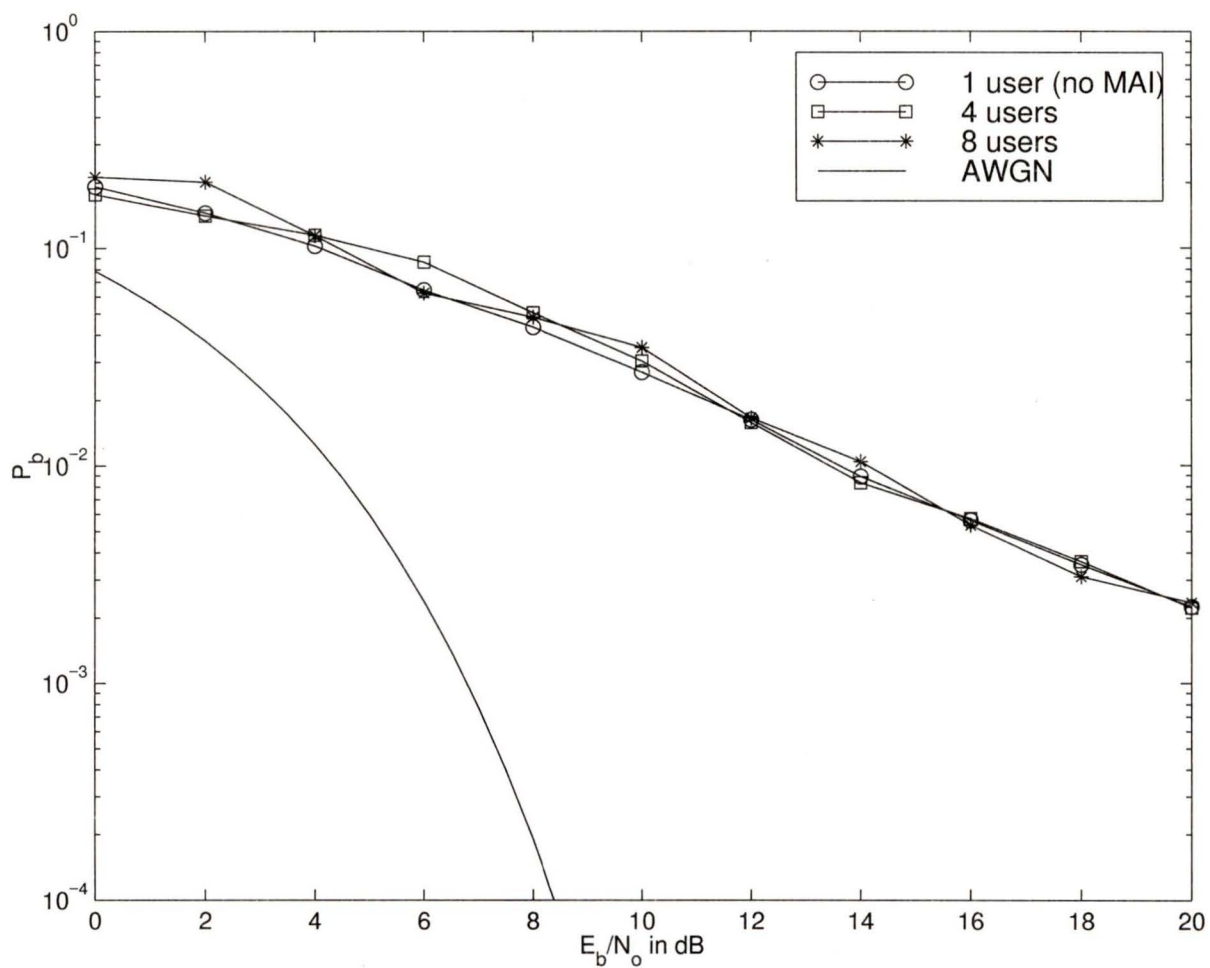


Figure 4.4. Results for inverse equalization (INV).

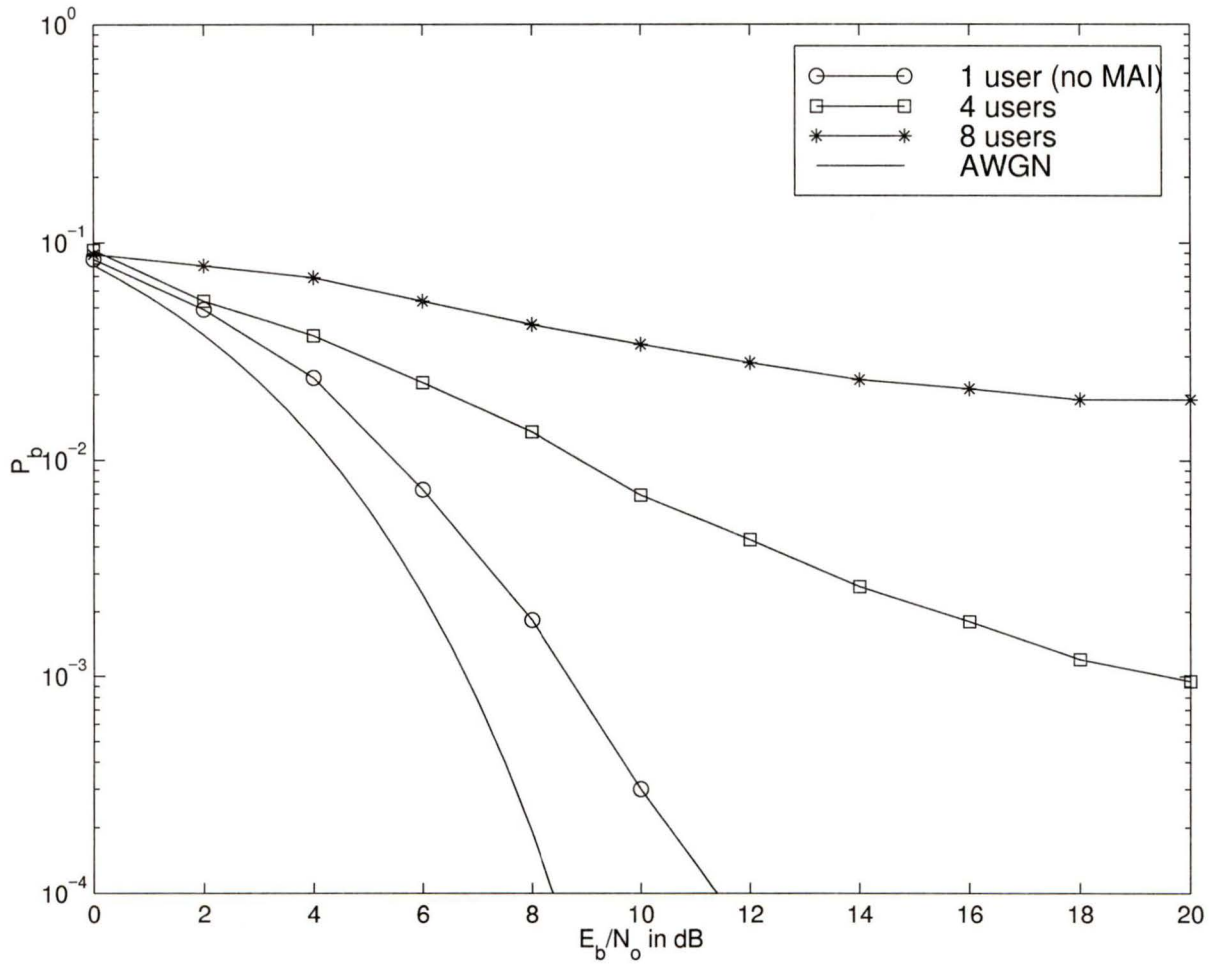


Figure 4.5. Results for Equal Gain Combining (EGC) equalization.

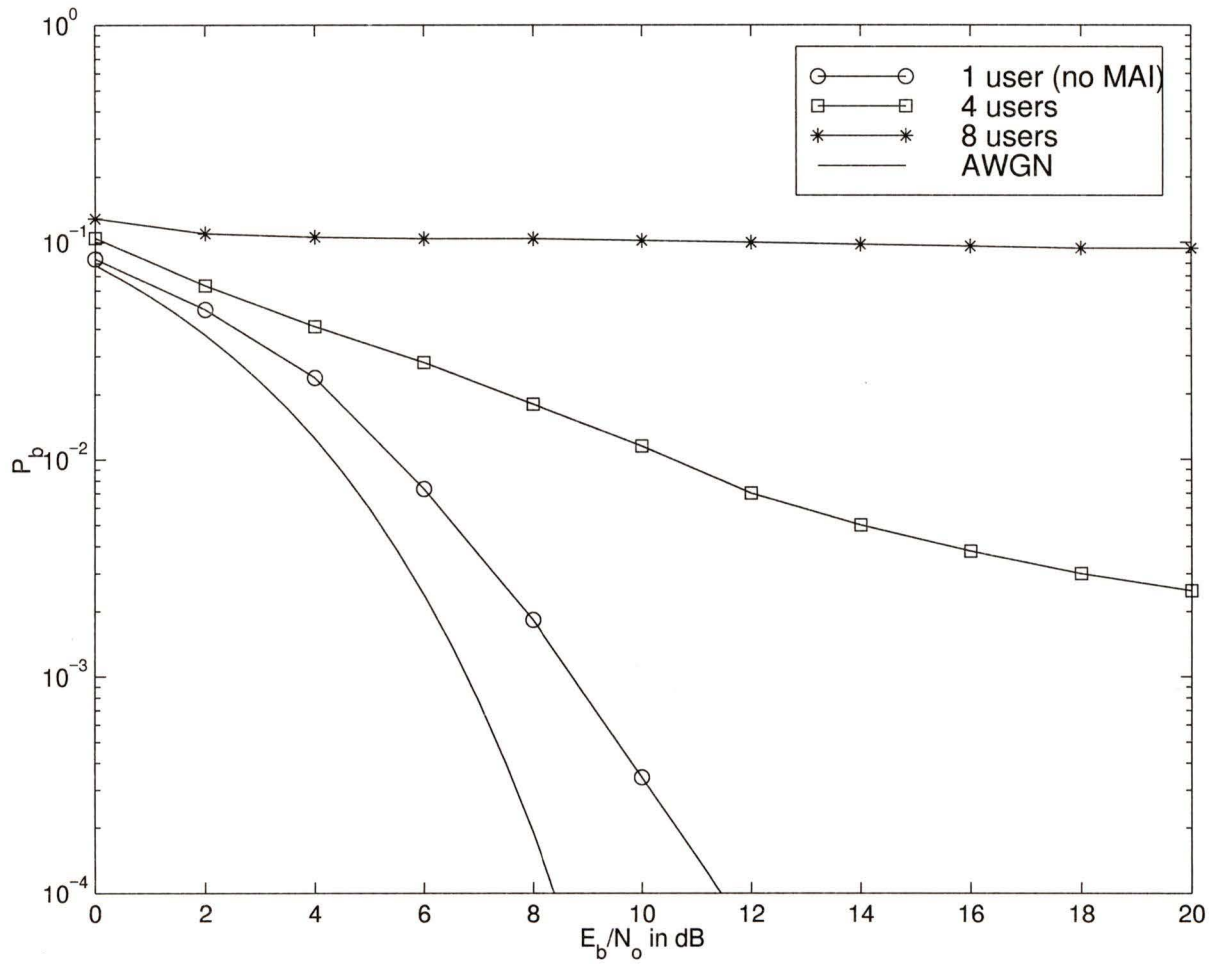


Figure 4.6. Results for Maximum Ratio Combining (MRC) equalization.

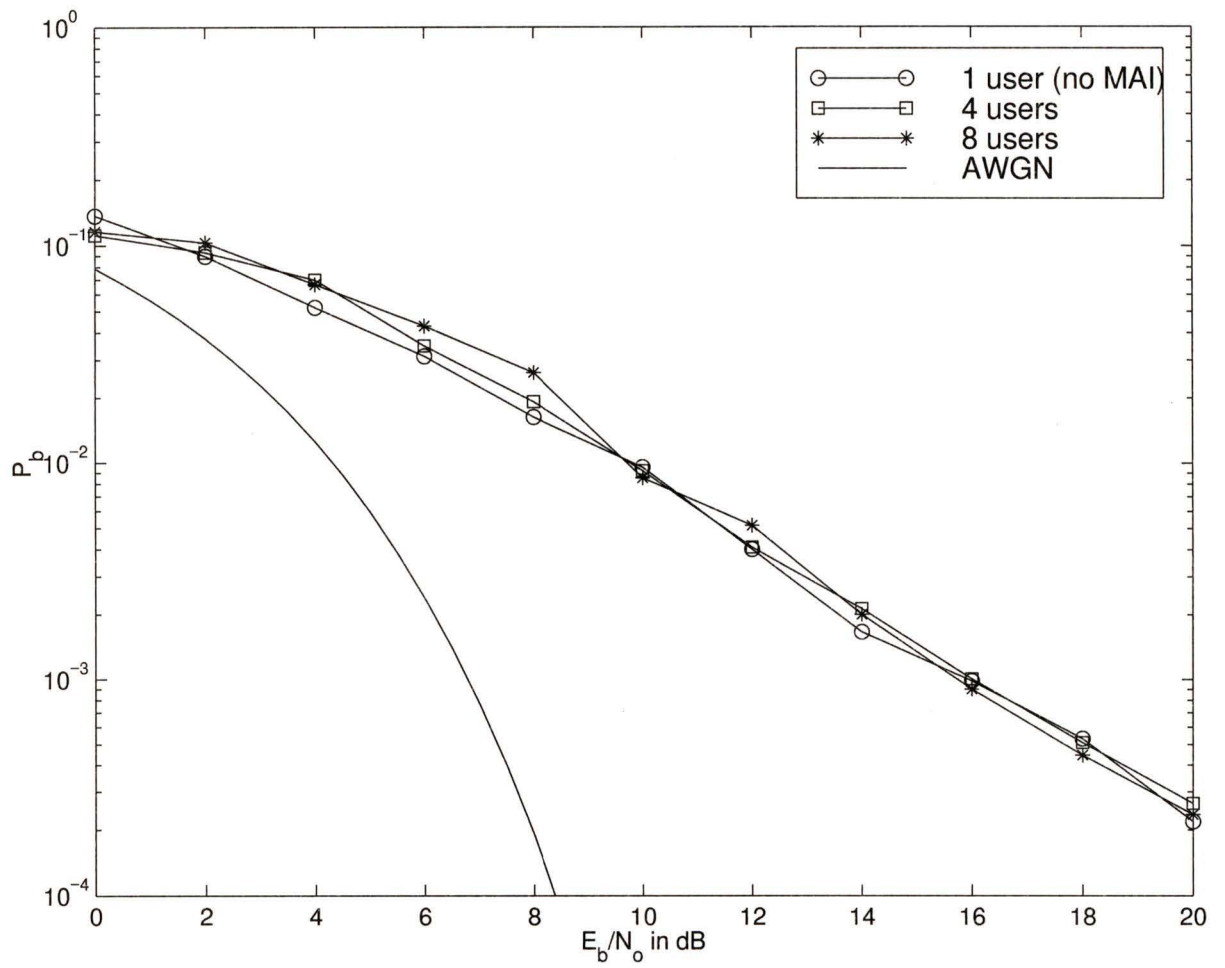


Figure 4.7. Results for Controlled Equalization (CE) with $\rho = 0.4$.

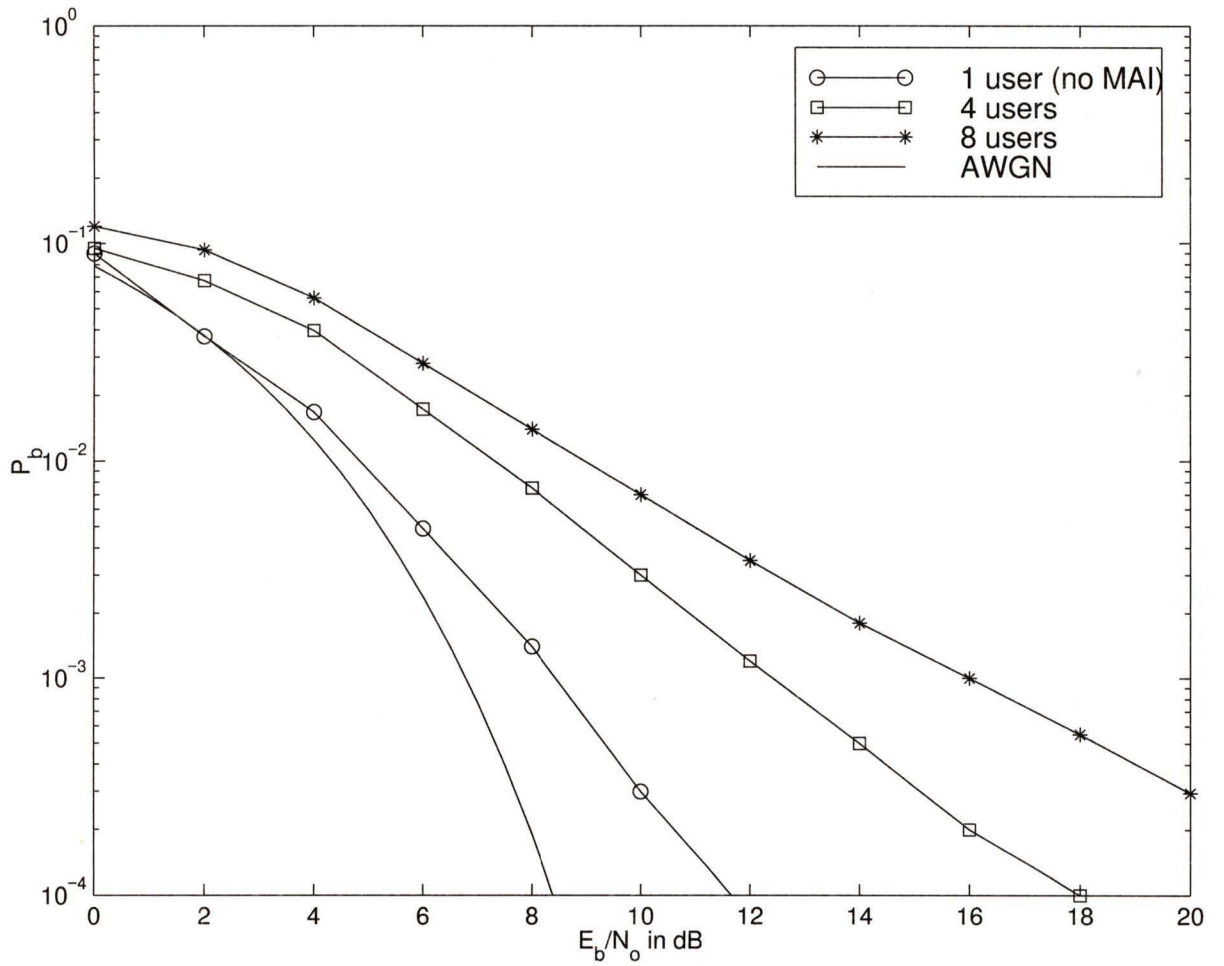


Figure 4.8. Results for Minimum Mean Square Error (MMSE) equalization.

4.2.2 Interference Cancellation

In order to perform interference cancellation the number of active users must be known as well as all active user spreading codes. The MMSE technique performs well for high numbers of active users, thus it is a suitable choice for the first detection. In the following detection MAI is reduced, corresponding to the transmission of fewer active users. For this case both EGC and MMSE are evaluated. MMSE equalization can also perform well for low numbers of users but it requires accurate information about the number of remaining interferers after interference cancellation. The number of remaining interferers can only be coarsely approximated; if it is incorrect, then other methods, such as EGC, may perform better [30]. With the addition of soft interference cancellation performance improves due to a reduction in error propagation. The performance of the two schemes are given in Figure 4.9.

Figure 4.9 includes the simulation results for MLD with full capacity of 8 users per user group and spreading code length $L = 8$. It can be seen that the performance is slightly inferior to multi-user detection with MMSE. This result is significant in that MLD requires much higher complexity than MUD. However, without knowledge of the number of active users MUD cannot be employed.

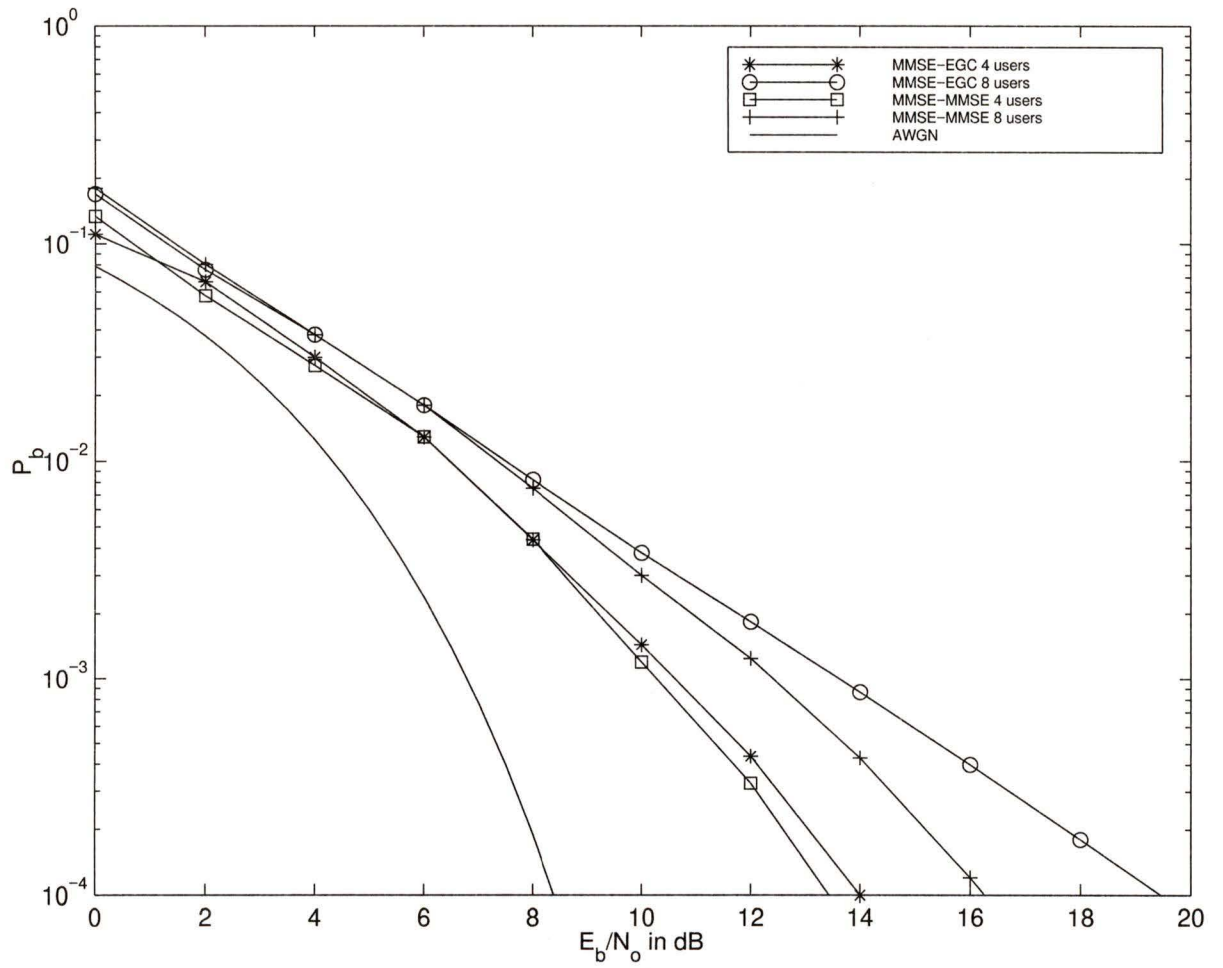


Figure 4.9. Results for Multi-User Detection (MUD) equalization.

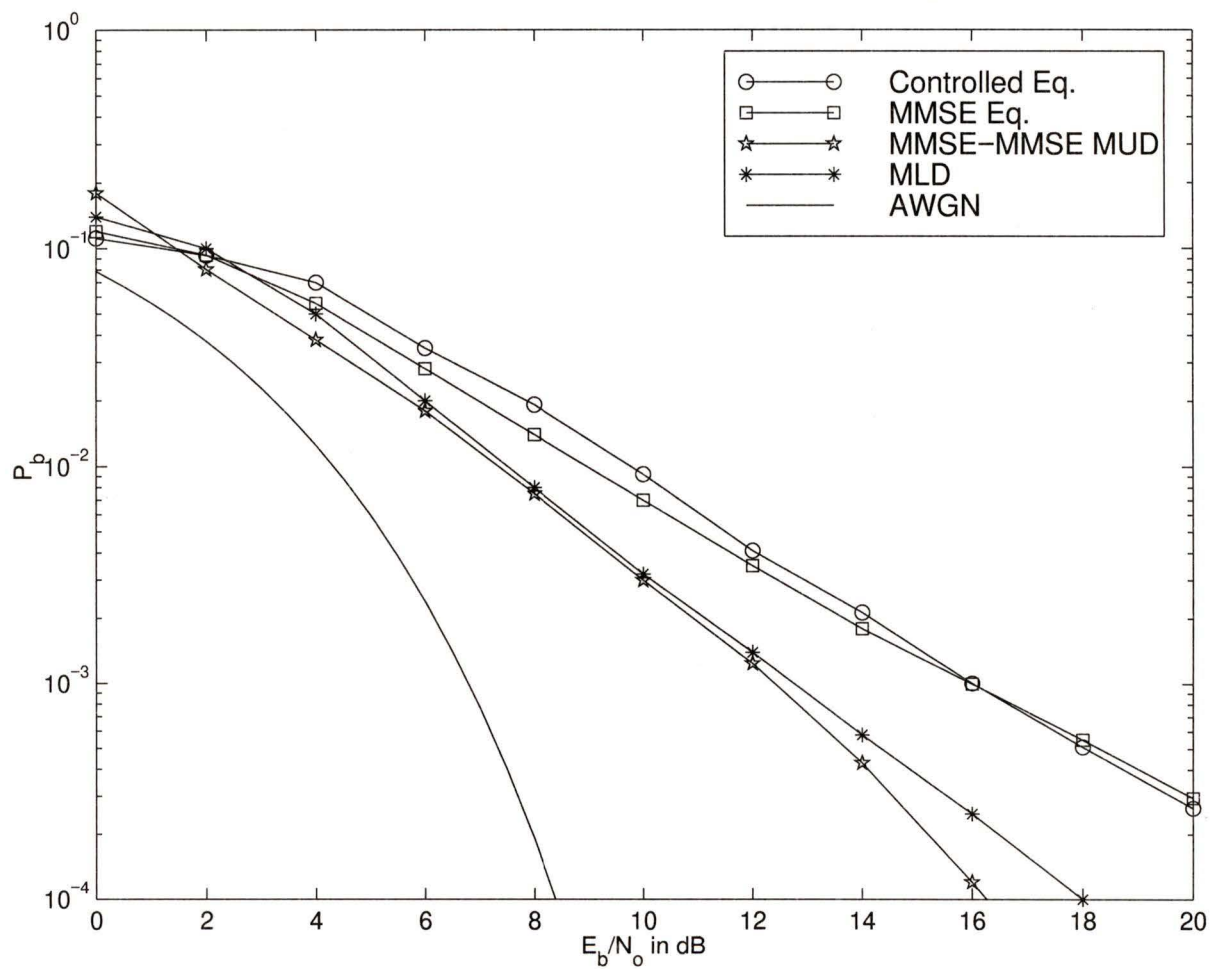


Figure 4.10. A comparison of the best equalization schemes for system of varying complexity.

4.3 Summary

Figure 4.10 indicates the best equalization choice for low and high complexity receivers. A drawback of using controlled equalization is that it gives similar performance for all traffic levels. MMSE equalization, on the other hand, requires knowledge of the number of active users. The best performance was achieved using MMSE-MMSE MUD, which outperforms MLD even at much lower complexity.

Table 4.1 provides a measure of complexity and minimum SNR requirements. The normalized number of floating point operations per detected MC-CDMA symbol is used to measure complexity. Since channel coding is not taken into account, we focus on bit error probability in the range $BER = 10^{-3}$.

Table 4.1. Normalized complexity and $BER = 10^{-3}$ performance of detection schemes

Method	Normalized complexity	SNR (dB)
Controlled Eq	.371	16
MMSE Eq	.373	15.4
MUD	.5	12.5
MLD	1	12.8

4.4 Channel Coding

In this section the use of channel coding on the MC-CDMA system is considered. As these results are obtained primarily to illustrate the BER performance achievable for a practical implementation, an in-depth investigation of channel coding is not carried out.

Convolutional codes with a maximum likelihood Viterbi decoder are used [10]. Each data bit d_i , $i = 1 : N_u$, has duration T_d . The N_u data bit streams are convolutionally encoded with code rate $R = K/N$, where N is the output sequence length. The input to the decoder is a sequence d^i of length K . The output of the encoder is the encoded bit sequence b^i of length N . The duration of a single code bit is $T_b = RT_d$ which corresponds to a chip duration of $T_c = T_b/L$. A frame length of 24 MC-CDMA symbols is chosen. This limits the delay time to 10ms which is much less than the maximum preprocessing delay allowable for voice communications. The coded MC-CDMA scheme is considered for MMSE

equalization and MLD. For MMSE the only difference in Equation 4.15 is that the SNR is determined as E_s/N_o where E_s is the average energy of the received code bits.

The main advantage of the Viterbi algorithm is its ability to exploit soft decision information. In the previously discussed coded system only hard decision data was used in the Viterbi decoder. To obtain this advantage soft values must be provided to the channel decoder. The optimum soft value for the Viterbi algorithm is the log-likelihood ratio, Λ . The log-likelihood ratios for MC-CDMA systems with MMSE and with MLD are derived in [31].

For coded bit b^j of user j , $j = 1 : N_u$ at the output of the channel encoder for MC-CDMA systems with equalization the log-likelihood ratio can be simplified as

$$\Lambda^j \approx \frac{4E_s}{N_o} v^j, \quad \text{if } L \gg 1, \quad (4.19)$$

where $v^j = (\vec{u}, c^j)$ is the soft decision variable assigned to bit d^j of user j . For short spreading code lengths with the use of MMSE, it has been found in [30] that somewhat better results can be obtained using

$$\Lambda^j \approx \frac{4E_s}{N_o} v^j \sum_{l=1}^L h_l \quad (4.20)$$

It should be noted however, that Equation 4.20 performs much worse than Equation 4.19 for other equalization techniques.

For MLD the log-likelihood ratio for MC-CDMA with MLD can be approximated as

$$\Lambda^j \approx \frac{E_s}{N_o} (\delta_{I'}^2 - \delta_{I''}^2), \quad (4.21)$$

where I' is the index of the possible sequence with the smallest squared Euclidean distance δ^2 where $b^j = -1$ and I'' is the index of the possible sequence with the smallest squared Euclidean distance δ^2 where $b^j = +1$.

Convolutional interleaving should be used in place of the block interleaver in this case. Convolutional interleavers are better matched for use with convolutional codes [10]. For the results presented in Figure 4.11, however, the low complexity block code of Section 3.6.2 is used.

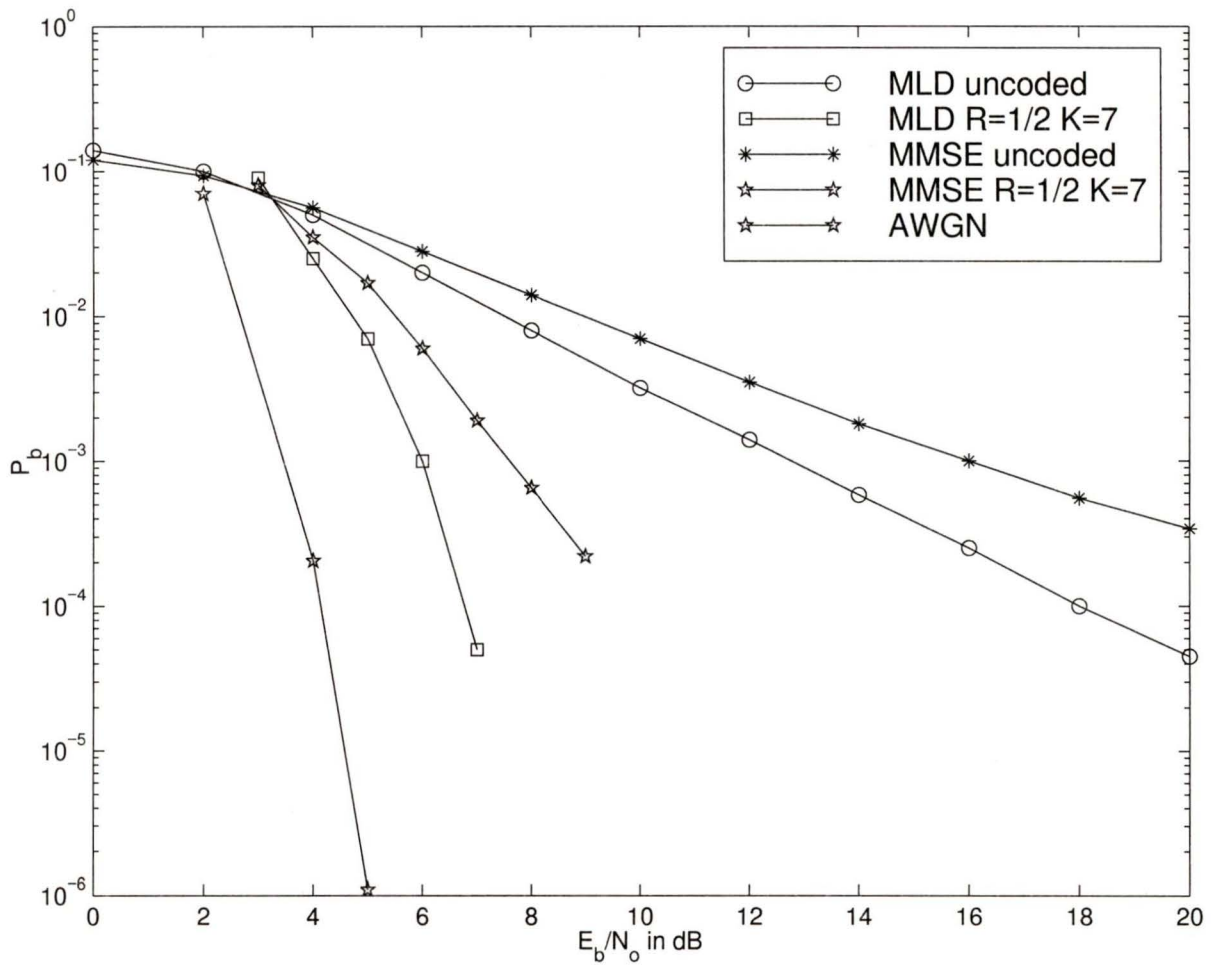


Figure 4.11. Rate 1/2, K=7, convolutionally encoded MC-CDMA with MLD and MMSE.

4.5 Spreading Codes for Crest Factor Reduction

The peak to average power ratio (or crest factor) measures the extent of fluctuation of maximum signal power over time. The reduction of crest factor (CF) is a critical issue in the design of a MC-CDMA system. Due to the statistical independence of the subcarriers, the corresponding time-domain samples $s_i(t)$, $i = 1 : N_c$ are approximately Gaussian distributed. This results in a high crest factor

$$CF = \frac{\max_i\{|s_i(t)|^2\}}{E\{|s_i(t)|^2\}} \quad (4.22)$$

Because multi-carrier systems are bit synchronous there are a limited range of possible transmitted waveforms. This implies that the sequences with high crest factor will occur more frequently than in an unsynchronized system such as DS-SS-SSMA. Signals with high crest factors may overload nonlinearities in amplifiers designed to accommodate the average signal power but not the extreme values that occur in multi-carrier systems. This overload causes intermodulation among subcarriers and, more importantly, undesired out-of-band radiation. RF amplifiers that operate without large power backoff will not be able to keep the out-of-band radiation below specified limits. This leads to inefficient amplification and expensive transmitters.

Another consideration for code selection is frequency distribution. By spreading user bits across many subcarriers fading resistance is improved. To retain this advantage it is therefore desirable to select spreading codes that result in even power distribution across the subcarriers.

A subcarrier sequence with ideal crest factor satisfies the following relationship

$$|s(t)|^2 = \text{constant} \quad (4.23)$$

where $|s(t)|^2$ is the time domain signal power. The Fourier transform of this relationship gives

$$R(f) = \delta(f) \quad (4.24)$$

where $R(f)$ is the autocorrelation function of the frequency domain sequence $S(f)$, corresponding to $s(t)$, and δf is an impulse response in the frequency domain. A trivial solution to 4.24 would be an impulse in the frequency domain. This type of signal exhibits poor

fading performance because the signal will be concentrated in a single diversity branch. To maximize the advantages of frequency diversity an additional requirement

$$|S(f)|^2 = \text{constant} \quad (4.25)$$

can be added. These requirements severely limit the type of codes that can be chosen. In most cases one of the requirements must be ignored in order to satisfy the others. Furthermore, the objective of minimizing crest factor often conflicts with other objectives such as Rayleigh fading performance and spectral efficiency.

Orthogonal WH codes were chosen at the outset for our system for the simple receiver structures they allow. Orthogonal codes have zero cross-correlation when perfectly equalized, thus eliminating multiple access interference. Such codes allow for simple correlation receivers where each user can detect their data with no information required about other users. WH codes also produce low crest factors. Referring to Equation 4.33, each code word of the WH matrix can be viewed as a unique frequency component. These frequencies range from DC (all elements equal valued) to the highest frequency component (alternating antipodal values). Summing these codes results in an even frequency domain distribution, or in the case of MC-CDMA an even time domain distribution which results in low crest factor signals.

In selecting WH codes the requirement of Equation 4.25 must be relaxed, resulting in some codes which give rise to subcarrier sequences with poor frequency distribution. With WH codes a subset of these sequences will be impulses. For example, if L users each send a sequence of ones the corresponding subcarrier sequence is

$$\vec{s} = [\sqrt{L}, 0, \dots, 0, 0] \quad (4.26)$$

while all minus ones results in

$$\vec{s} = [\sqrt{-L}, 0, \dots, 0, 0] \quad (4.27)$$

Thus, the entire Euclidean distance between subcarrier sequences is contained in one diversity branch. In a fading channel the incorrect detection of this sequence would result in the maximum number of errors, L . The performance of these sequences are inferior to those of the rest of the set.

Multi-user detection (MUD) enables the use of near-orthogonal codes. Near orthogonal

codes are designed to minimize cross correlation while optimizing for another design criterion. If optimized for reduced crest factor then performance superior to orthogonal codes can be achieved. The added MAI caused by near orthogonal codes is removed by MUD with interference cancellation to achieve the same spectral efficiency as orthogonal codes, albeit with increased receiver complexity. The advantage of this type of code is that it increases the flexibility in code selection where some orthogonality can be sacrificed to achieve a lower crest factor.

If maximum likelihood detection is employed then there is no longer a strong advantage in choosing orthogonal codes. The Euclidean distance between subcarrier sequences is large and constant between all possible sequences when using WH codes; however, the frequency distribution of the sequences varies greatly as seen in the previous example.

Subcarrier sequences formed by orthogonal codes can be considered as a sum of overlapping code sequences. In MLD each subcarrier sequence is treated as a unique symbol that represents the data from all users. The received sequence is compared to all possible sequences to determine the sequence which was most likely transmitted. This allows for the maximum flexibility in designing spreading codes to shape the desired waveform. This flexibility, however, is gained at the expense of increased complexity. When using MLD in a fading environment the subcarrier sequences should be designed in such a way as to maximize the Euclidean distances over all subcarriers.

If low complexity receivers are a high priority in system design, then correlation receivers with orthogonal codes should be chosen. Although WH codes exhibit good crest factor performance [32] several methods exist to reduce it further. One method of reducing the crest factor without altering the orthogonality of the codes is by increasing the code length L . Increasing L has the effect of spreading the power in time which decreases crest factor. Lengthening the codes can be easily accommodated without increasing the number of subcarriers by appropriate scaling of the number of user groups although with a corresponding increase in complexity.

4.5.1 Phase Rotation

Another method for crest factor reduction is through phase rotation [33]. Phase rotation can assure that the subcarriers are never all in-phase while orthogonality of the spreading codes is maintained. Applying the phase rotations

$$\phi_i = i \frac{\pi}{L}, \quad i = 0 : L \quad (4.28)$$

to the WH code matrix, where i represents the code of user i , the code elements become complex while maintaining orthogonality with respect to the other codes. The spreading code matrix then becomes

$$C = \begin{bmatrix} c_0^0 \phi_0 & c_1^0 \phi_0 & \cdots & c_{L-1}^0 \phi_0 \\ c_0^1 \phi_1 & c_1^1 \phi_1 & \cdots & c_{L-1}^1 \phi_1 \\ \vdots & \vdots & \ddots & \vdots \\ c_0^{L-1} \phi_{L-1} & c_1^{L-1} \phi_{L-1} & \cdots & c_{L-1}^{L-1} \phi_{L-1} \end{bmatrix} \quad (4.29)$$

Besides reducing the crest factor, applying phase rotation to the spreading codes can also improve the frequency distribution if chosen properly. By distributing the Euclidean distances over a larger number of subcarriers, phase rotation also more evenly distributes the signal in the frequency domain. The effect of this can be seen in Figure 4.12 as a significant improvement in BER performance. In this case phase rotations of $i\pi/L$, $i = 1 : L$ are used with MMSE equalization to achieve a 1.5 dB gain at BER = 10^{-3} . Figure 4.13 displays the pdf of Euclidean distances for subcarrier sequences with and without the phase rotation specified above. While phase rotation spreads the Euclidean distances across more subcarriers, it is clear from Figure 4.13 that the expected value of the Euclidean distances have decreased. Thus, phase rotation of spreading codes improves equalizer performance, but is not recommended for use with systems using MLD.

Another method of employing phase rotations is to apply them to the K subcarrier sequences of length L [34]. The orthogonal codes reduce crest factor caused by L subcarrier elements while phase rotation minimizes crest factor caused by potentially K identical copies of the same subcarrier sequence.

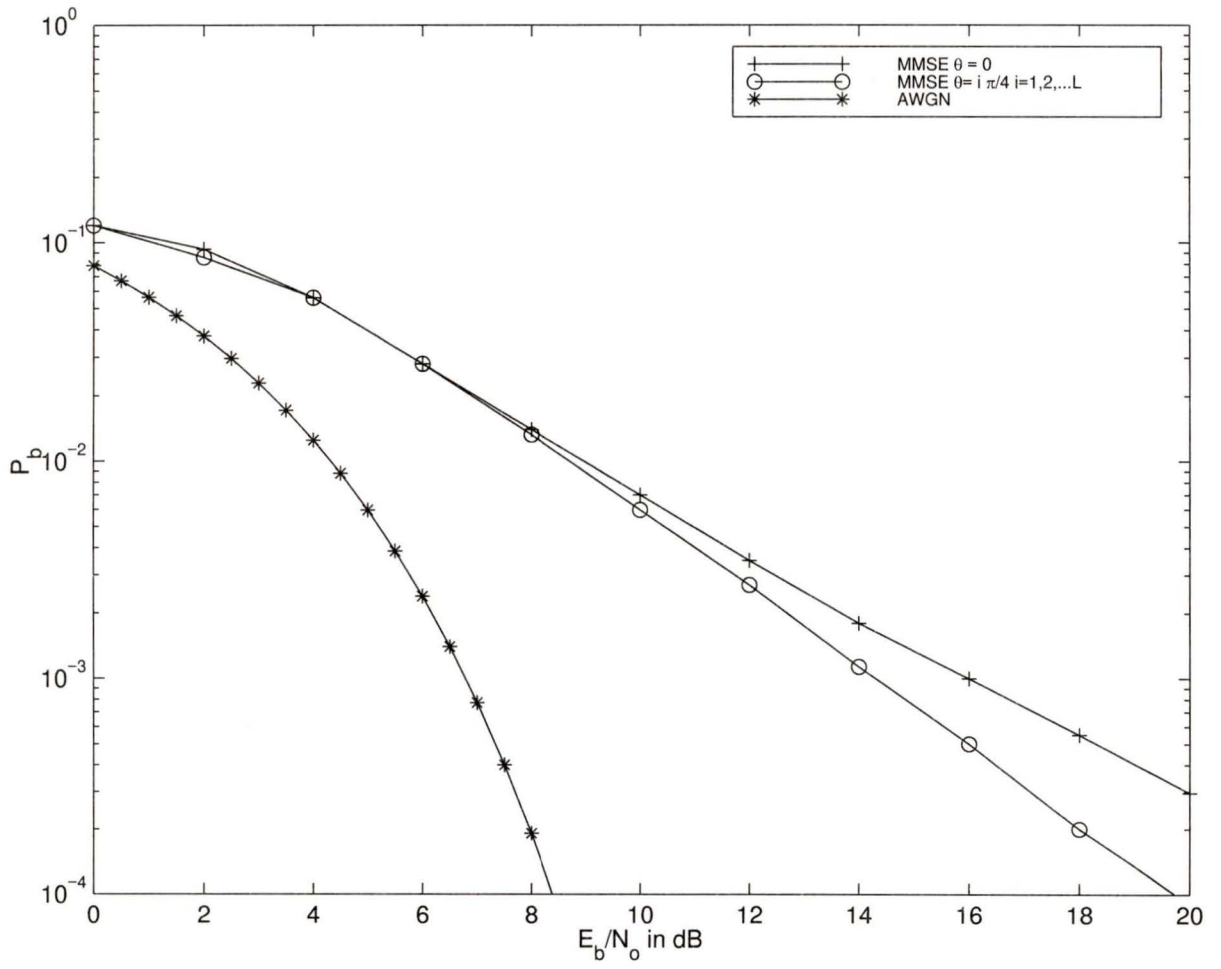


Figure 4.12. Applying phase rotation to spreading codes.

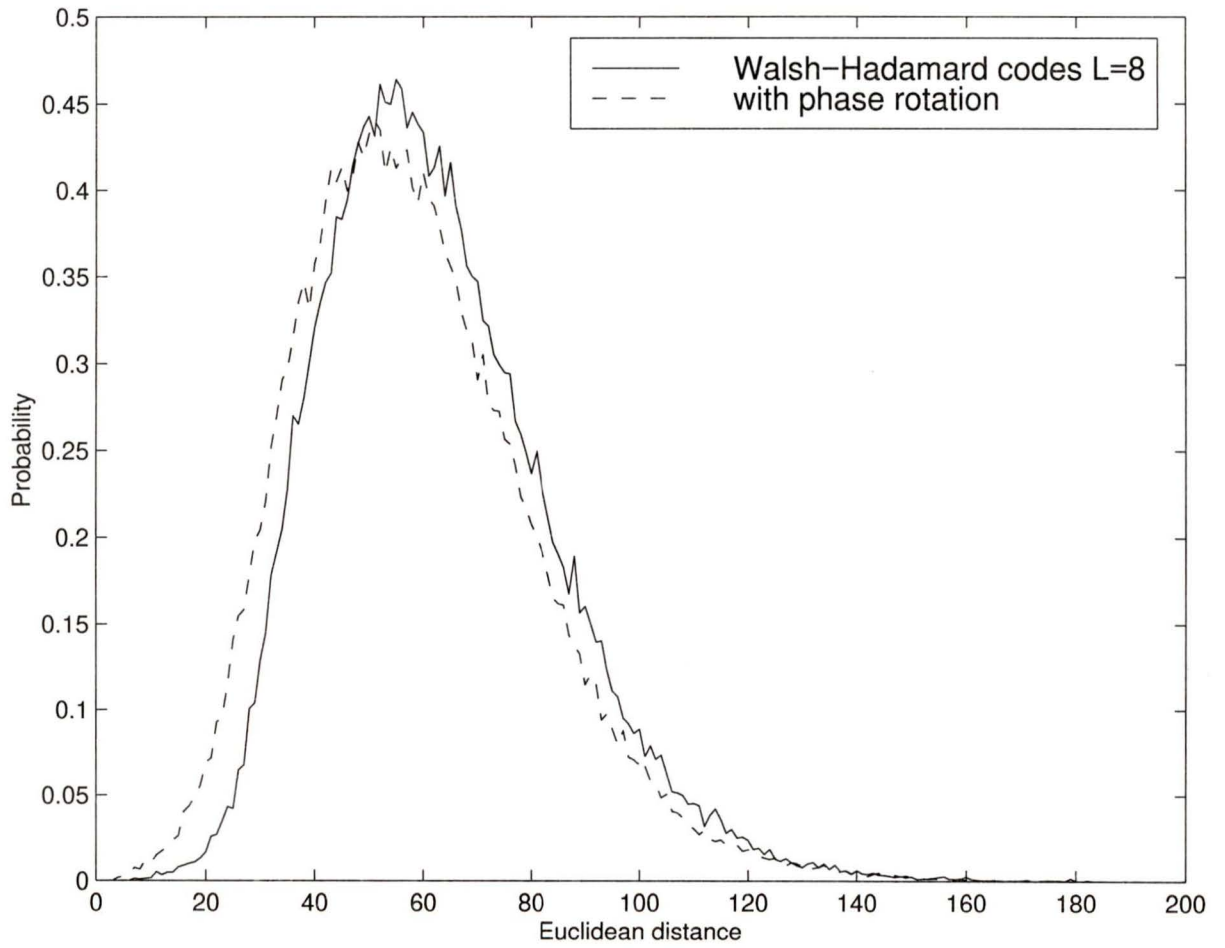


Figure 4.13. Normalized probability density function of Euclidean distances of received vectors about the transmitted vector.

4.5.1.1 Phase Scrambling

Rather than applying a fixed set of phase rotations to the codes or to the subcarrier sequence itself, a random set of phase rotations may be applied [35, 36, 37]. This uncoordinated approach has the advantage of simplicity and can lead to considerable reduction in crest factor. The following section details one method of applying phase scrambling to an MC-CDMA system with low complexity.

4.6 Selected Mapping (SLM)

We assume that both the real and imaginary components of the time-domain samples of the subcarriers $s_n(t)$, $n = 1 : N_c$ are identically and independently Gaussian distributed. The probability that the crest factor of the MC-CDMA symbol exceeds a threshold Y , or

$$|s_n(t)|^2 > YE\{|s_n(t)|^2\} \quad (4.30)$$

is given by:

$$\Pr\{CF > Y\} = 1 - (1 - e^{-Y})^{N_c} \quad Y > 0 \quad (4.31)$$

Equation 4.31 assumes there is only one subcarrier sequence available to represent the transmitted information. However, if M statistically independent MC-CDMA symbols can be found that represent the same information then the symbol with the lowest CF is chosen from the set of M and the probability that CF_{lowest} exceeds Y is given by

$$\Pr\{CF_{lowest} > Y\} = (1 - (1 - e^{-Y})^{N_c})^M \quad Y > 0 \quad (4.32)$$

Equation 4.32 represents the complimentary cumulative distribution function of CF . Figure 4.14 gives the probability of that lowest CF out of $M = 2^m$, $m = 0 : 3$ possibilities is greater than Y with N_c . It is clear that for increasing M the probability of $CF > Y$ decreases dramatically.

To generate M signals representing the same information, M distinct vectors are defined $\vec{P}^m = [P_1^m, \dots, P_{N_c}^m]$, where $P_n^m = e^{j\phi_n^m}$ and $\phi_n^m \in [0, 2\pi]$, $n = 1 : N_c$, $m = 1 : M$. The subcarrier sequence \vec{S} is now multiplied carrier wise with each of the M vectors \vec{P}^m , resulting in a set of M different MC-CDMA symbols

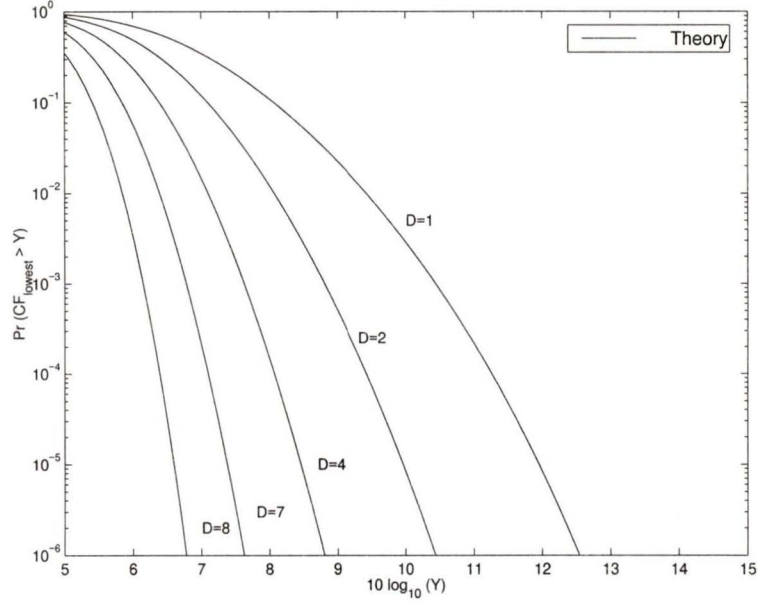


Figure 4.14. Complimentary cumulative distribution function of CF if MC-CDMA symbol with lowest CF is selected out of M statistically independent symbols.

$$\vec{S}^m = s_n e^{j\phi_n^m} \quad n = 1 : N_c, \quad m = 1 : M \quad (4.33)$$

After all M MC-CDMA symbols have been transformed into the time domain the one with the lowest CF is selected for transmission. Depending on the implementation, side information may be required to specify which P^m was used. Sending the selected phase sequence m will require channel coding to ensure this number is received correctly. Another possible method to recover the data is to have M channels process the received signal in parallel. Each decoder employs one vector P^m . The most probable result is used to detect the user data.

Simulations results for our MC-CDMA system with the number of subcarriers per user group $N_g = N_c/Q = 64$ and $M = 4$ are given in Figure 4.15. The vectors \vec{P}^m are randomly generated with $P_n^m \in [\pm 1, \pm j]$. By using only phase shifts of multiples of $\pi/2$ they can be implemented without any multiplications. It can be seen in Figure 4.15 that selected mapping significantly reduces probability of high crest factor in the simulated system even with $M = 4$. This improvement is gained with only a slight increase in system complexity. Another advantage of this technique is that it removes some of the burden of crest factor reduction from the spreading codes. This implies that the emphasis in spreading code

selection can be shifted toward achieving good performance in a fading channel.

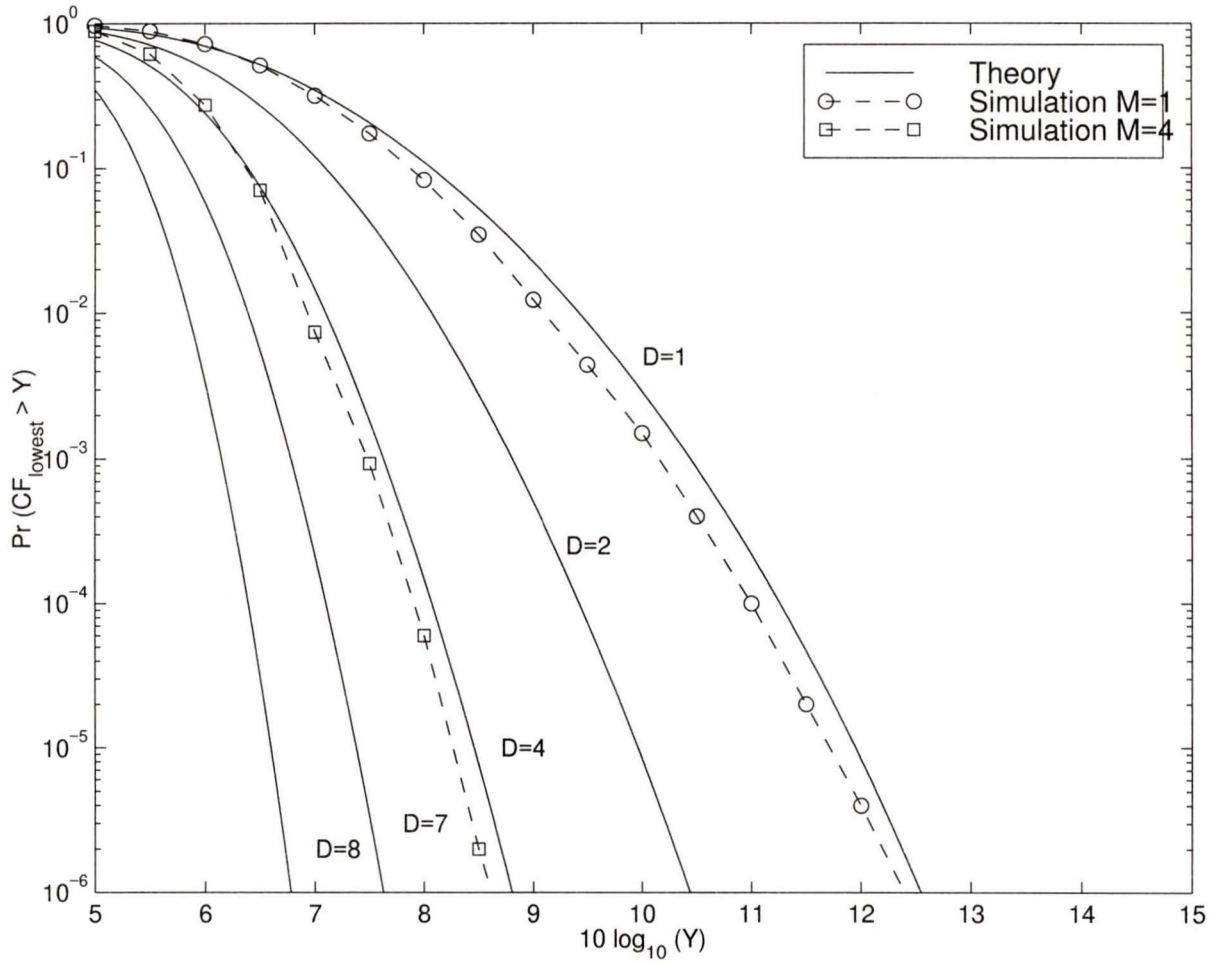


Figure 4.15. Complimentary cumulative distribution function of CF_{lowest} with $M=1$ and 4, $D=512$.

Chapter 5

Conclusions and Suggestions for Further Work

5.1 Conclusions

MC-CDMA is a hybrid multiple access technique that has recently gathered interest for its application in the next generation of mobile wireless communication networks. The environment of interest for these networks is one in which the signal experiences fast and slow frequency selective fading.

In Chapter 3 a typical bad urban mobile radio channel profile is selected for the selection of system parameters. Parameters based on this channel were selected with consideration of system performance and complexity while maintaining the required conditions of slow flat fading subcarriers. A spreading code of length $L = 8$ was chosen based on achieving the maximum possible frequency diversity for the selected environment with minimum code length. To accommodate a short code length user groups were introduced with a subsequent reduction in multiple access interference with proper channel assignment. User groups are also shown to increase system flexibility in terms of trading capacity for user data rates. Block interleaving was implemented for the investigation of single cell performance although slow frequency hopping may be applied to the interleaver in the multi-cell environment. To obtain estimates of the channel transfer function for each subcarrier, two-dimensional channel estimation was investigated. Channel estimates are required if equalization is to be performed. The two dimensional estimation makes use of residual frequency and time correlation between adjacent subcarriers to enable a 2-D grid of pilot tones to be determined. Interpolation between the maximally spaced pilot tones gives channel estimates for all subcarriers.

Chapter 4 makes use of the system parameters determined in the previous chapter for creating a simulation of the MC-CDMA system downlink. The bit error rate performance curves for a variety of detection schemes are simulated. These schemes included conventional equalization schemes, such as equal gain combining and maximum ratio combining. The controlled equalization technique introduced gives superior performance to maximum ratio combining, equal gain combining, and inverse equalization. The conventional detection scheme that provided the best performance was shown to be minimum mean squared error equalization. For improved performance, multi-user detection with interference cancellation was investigated. Of the two schemes investigated the method using minimum mean squared error for both interference cancellation and final detection proved to have the best performance. Finally, maximum likelihood detection was investigated. This scheme was shown to have performance similar to that of the multi-user detection schemes, however it requires no information about the number of active users or their spreading codes. The performance of all techniques presented in terms of uncoded bit error rate and relative complexity illustrates that maximum likelihood detection has by far the highest level of receiver complexity.

A simulation of MC-CDMA with channel coding was presented next. Channel coding will be required for any practical system in order to achieve the bit error rates required for most data applications. Results were given for maximum likelihood detection and minimum mean squared error equalization. The results obtained were in agreement with performance expected from the literature.

In the following section the selection of spreading codes was considered with respect to the crest factor and the frequency distribution of the transmitted MC-CDMA symbol. Techniques for crest factor reduction were discussed for conventional, multi-user, and maximum likelihood detection. Coordinated phase rotation was shown to reduce crest factor for the minimum mean squared error detection scheme and can be applied to any of the conventional techniques evaluated. In the case of conventional detection, improved bit error rate performance is a result of wider frequency distribution of the signal. Finally, a scheme which makes use of phase scrambling was presented; referred to as Selected Mapping (SLM) the technique was shown to have significant improvement in crest factor performance while not significantly decreasing the Euclidean distances between subcarrier sequences. Analytical results were provided as well as simulation results for one and four phase scrambling vectors. The results indicate that this method can reduce the probability of high crest factor with only a moderate increase in complexity.

5.2 Suggestions for Further Work

MC-CDMA is a new multiple access scheme that has yet to be proven in a real world mobile radio applications. As such there exists still several problems related left to be addressed.

In this work perfect chip synchronization was assumed. Removing this assumption will allow investigation of the sensitivity of MC-CDMA to chip timing jitter (or chip synchronization error). Investigation into the effect of timing error about the sampling period and subsequent research into mitigation techniques are needed. One suggestion [38], is to use convolutional coding with automatic repeat request (ARQ) to compensate for the bit error rate degradation produced by both chip timing jitter and fading.

The use of adaptive signal alphabets for OFDM is suggested in [1]. Further research in this area is required to determine if the increased data rates possible with adaptive modulation can be applied to MC-CDMA in the mobile radio channel. This would be an interesting area for follow-up research.

References

- [1] A. Czylik, "OFDM and related methods for broadband mobile radio channels," in *Intl. Zurich Seminar on Broadband Communications*, Feb 1998, pp. 91–98.
- [2] T. Rappaport, *Wireless Communications: Principles and Practice*, Prentice-Hall, New Jersey, 1996.
- [3] H. Leib P. Mermelstein, A. Jalali, "Integrated services on wireless multiple access networks," in *Proc. IEEE ICC '93*, 1993, pp. 863–867.
- [4] N. Yee, J-P. Linnartz, and G. Fettweis, "Multicarrier CDMA in indoor wireless radio networks," in *Proc. Int. Symp. on Personal, Indoor and Mobile Radio Commun. (PIMRC'93)*, Sept 1993, pp. 109–113.
- [5] W.C. Lee, *Mobile Communications Design Fundamentals*, Wiley, New York, 1993.
- [6] M. D. Yacoub, *Foundations of Mobile Radio Engineering*, CRC Press, Ann Arbor, 1993.
- [7] D. E. Borth R. L. Peterson, R. E. Ziemer, *Introduction to Spread Spectrum Communications*, Prentice-Hall, New Jersey, 1995.
- [8] K.S. Gilhousen, I.M. Jacobs, R. Padovani, A.J. Viterbi, L.A. Weaver, and C.E. Wheatley, "On the capacity of a cellular CDMA system," in *IEEE Trans. Veh. Tech. (VTC'91)*, May 1991, vol. vol. 4, pp. 303–312.
- [9] K. Fazel and L. Papke, "On the performance of convolutionally-coded CDMA/OFDM for mobile communication systems," in *Proc. Int. Symp. on Personal, Indoor and Mobile Radio Commun. (PIMRC'93)*, Sept 1993, pp. 468–472.
- [10] J. G. Proakis, *Digital Communications, third ed.*, McGraw-Hill, New York, 1996.
- [11] J. A. C. Bingham, "Multicarrier modulation for data transmission: An idea whose time has come," in *IEEE Communications Magazine*, May 1990, pp. 5–14.
- [12] S.B. Weinstein and P.M. Ebert, "Data transmission by frequency division multiplexing using the discrete Fourier transform," in *IEEE Trans. Commun. Tech.*, Oct 1971, vol. COM-19, pp. 628–634.
- [13] M. Alard and R. Lasalle, "Principles of modulation and channel coding for digital broadcasting using the discrete Fourier transform," in *EBU Review, Technical No. 224*, Aug 1987, pp. 47–69.

- [14] J.S. Chow, J.C. Tu, and J.M. Coiffi, "A discrete multitone transceiver system for HDSL applications," in *IEEE Journal on Selected Areas in Commun. (JSAC)*, 1991, vol. 9, pp. 895–908.
- [15] ETS 300 401 ETSI, "Radio broadcast systems: digital audio broadcasting (DAB) to mobile, portable and fixed receivers," .
- [16] K. Fazel, S. Kaiser, P. Robertson, and M. Ruf, "A concept of digital terrestrial television broadcasting," in *Wireless Personal Communications*. 1995, vol. 2, pp. 9–27, Kluwer.
- [17] ETS 300 744 ETSI, "Radio broadcast system for television, sound and data services; framing structure, channel coding and modulation for digital terrestrial television," .
- [18] K. Fazel, S. Kaiser, and M. Schnell, "A flexible and high performance cellular mobile comm. system based on orthogonal multi-carrier SSMA," in *Wireless Personal Comm.* 1995, vol. 1, 2, pp. 121–144, Kluwer.
- [19] L. Vandendorpe, "Multitone spread spectrum multiple access communications system in a multipath Rician fading channel," in *Proc. IEEE Vehicular Tech. Conf. (VTC'95)*, July 1995, pp. 825–829.
- [20] G. Turin, "Introduction to spread-spectrum antimultipath techniques and their applications to urban digital radio," in *Proc. IEEE*, Mar 1980, vol. 68, pp. 328–353.
- [21] H. Sari, G.Karam, and I. Jeanclaude, "An analysis of orthogonal frequency division multiplexing for mobile radio applications," in *Proc. Vehicular Technology Conference (VTC'94)*, July 1994, pp. 1635–1639.
- [22] M. Failli, "Digital land mobile radio communications," in *Tech. Rep. COST 207*, 1989.
- [23] M. Schnell and S. Kaiser, "Diversity considerations for MC-CDMA systems in mobile communications," in *Proc. IEEE Fourth Int. Symp. on Spread Spectrum Techniques and Applications (ISSSTA '96)*, 1996, pp. 131–135.
- [24] Q. Chen, E. Sousa, and S. Pasupathy, "Multicarrier DS-CDMA with adaptive subcarrier hopping for fading channels," in *Proc. Int. Symp. on Personal, Indoor and Mobile Radio Commun. (PIMRC'95)*, 1995, pp. 76–79.
- [25] M.L. Moher and J.H. Lodge, "A time diversity modulation strategy for the satellite-mobile channel," in *Proc. 13th Biennial Symp. Comm.*, June 1986.
- [26] P. Hoeher, S. Kaiser, and P. Robertson, "Two-dimensional pilot-symbol-aided channel estimation by Wiener filtering," in *Proc. IEEE Int. Conf. on Acoustics, Speech and Signal Processing (ICASSP'97)*, Apr 1997, pp. 1845–1848.
- [27] P. Hoeher, *TCM on frequency-selective land-mobile fading channels*, Elsevier Science Publishers B.V., E. Biglieri, M. Luise (eds), 1992.
- [28] P. Hoeher, S. Kaiser, and P. Robertson, *Pilot-symbol-aided channel estimation in time and frequency*, Kluwer, K. Fazel, G.P. Fettweis (eds), 1996.

- [29] S. Kaiser, "Analytical performance evaluation of OFDM-CDMA mobile radio systems," in *Proc. European Personal and Mobile Commun. Conf. (EPMCC '95)*, Nov 1995, pp. 215–220.
- [30] S. Kaiser, "On the performance of different detection techniques for OFDM-CDMA in fading channels," in *Proc. IEEE Global Telecommun. Conf. (GLOBECOM'95)*, Nov 1995, pp. 2059–2063.
- [31] S. Kaiser, "Trade-off between channel coding and spreading in multi-carrier CDMA systems," in *Proc. IEEE Fourth Int. Symp. on Spread Spectrum Techniques and Applications (ISSSTA '96)*, Sept 1996, pp. 1366–1370.
- [32] V. Aue and G. Fettweis, "Multi-carrier spread spectrum modulation with reduced dynamic range," in *Proc. Vehicular Tech. Conf. (VTC'96)*, Apr 1996, pp. 914–917.
- [33] S. Boyd, "Multitone signals with low crest factor," in *IEEE Trans on Circuits and Sys.*, Oct 1986, vol. 33, pp. 1018–1025.
- [34] L. Freiberg, A. Annamalai, and V.K. Bhargava, "Crest factor reduction using orthogonal spreading codes in multi-carrier CDMA systems," in *Proc. Int. Symp. on Personal, Indoor and Mobile Radio Commun. (PIMRC'97)*, Sept 1997, pp. 120–124.
- [35] R.W. Baulm, R.F.H. Fischer, and J.B. Huber, "Reducing the peak-to-average power ratio of multicarrier modulation by selected mapping," in *Electronic Letters*, Oct 1996, vol. 32, no. 22, pp. 2056–2057.
- [36] M. Friese, "Multicarrier modulation with low peak-to-average power ratio," in *Electronic Letters*, Apr 1996, vol. 32, no.8, pp. 713–714.
- [37] S.H. Müller and J.B. Huber, "A comparison of peak power reduction schemes for OFDM," in *Proc. IEEE Global Telecommun. Conf. (GLOBECOM'97)*, Nov 1997, pp. 1–5.
- [38] L. Tomba and W.A. Krzymien, "Performance enhancement of multicarrier CDMA systems impaired by chip timing jitter," in *Proc. IEEE Fourth Int. Symp. on Spread Spectrum Techniques and Applications (ISSSTA '96)*, Sept 1998, pp. 136–140.

VITA

Surname: Marchildon Given Names: Guy, Denis
Place of Birth: Goose Bay, Newfoundland Date of Birth: July. 5, 1968

Educational Institutions Attended

Royal Military College of Canada	1987 to 1991
Dalhousie Technical University	1992 to 1993

Degrees Awarded

B.Eng	Royal Military College of Canada	1991
-------	----------------------------------	------

PARTIAL COPYRIGHT LICENSE

I hereby grant the right to lend my thesis to users of the University of Victoria Library, and to make single copies only for such users or in response to a request from the Library of any other university, or similar institution, on its behalf or for one of its users. I further agree that permission for extensive copying of this thesis for scholarly purposes may be granted by me or a member of the University designated by me. It is understood that copying or publication of this thesis for financial gain shall not be allowed without my written permission.

Title of Thesis: DESIGN CONSIDERATIONS IN MULTI-CARRIER CODE DIVISION MULTIPLE ACCESS.

Author: _____


GUY D. MARCHILDON

8 May 1998